

**EFFECT OF CROSS-ROLLING ON MICROSTRUCTURE, TEXTURE AND
MAGNETIC PROPERTIES OF COLD ROLLED NON-ORIENTED
ELECTRICAL STEELS**

A thesis submitted to the

National Institute of Technology Rourkela

In partial fulfilment of the requirements

Of the degree of

Masters of Technology

In

Metallurgical and Materials Engineering

By

Jitendra Kumar Mishra

(Roll no. 214MM2501)



DEPARTMENT OF METALLURGICAL AND MATERIALS ENGINEERING

NATIONAL INSTITUTE OF TECHNOLOGYROURKELA

**EFFECT OF CROSS-ROLLING ON MICROSTRUCTURE, TEXTURE AND
MAGNETIC PROPERTIES OF COLD ROLLED NON-ORIENTED
ELECTRICAL STEELS**

A thesis submitted to the
National Institute of Technology Rourkela

In partial fulfilment of the requirements

Of the degree of

Masters of Technology

In

Metallurgical and Materials Engineering

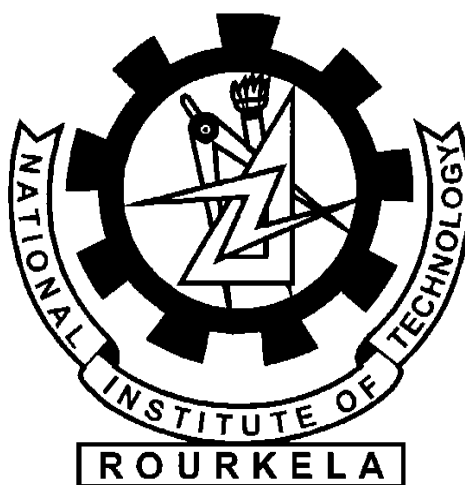
By

Jitendra Kumar Mishra

(Roll no. 214MM2501)

Under the supervision of

Prof. Santosh Kumar Sahoo



DEPARTMENT OF METALLURGICAL AND MATERIALS ENGINEERING

NATIONAL INSTITUTE OF TECHNOLOGYROURKELA

May, 2016



Department of Metallurgical and Materials Engineering
National Institute of Technology Rourkela

May 26, 2016

Certificate of Examination

Roll Number: 214MM2501

Name: Jitendra Kumar Mishra

Title of Thesis: Effect of cross-rolling on microstructure, texture and magnetic properties of cold rolled non-oriented electrical steels.

I, the below signed, after checking the dissertation mentioned above and the official record book(s) of the student, hereby state our approval of the dissertation submitted in partial fulfillment of the requirements of the degree of *Master Of Technology* in *Department of Metallurgical and Materials Engineering* at *National Institute of Technology Rourkela*.

I am satisfied with the volume, quality, correctness, and originality of the work.

.....

Prof. Santosh Kumar Sahoo

Principle supervisor



Department of Metallurgical and Materials Engineering
National Institute of Technology Rourkela

Prof. Santosh Kumar Sahoo

Department of Metallurgical and Materials Engineering

May 26, 2016

Supervisor's Certificate

This is to certify that the work presented in this dissertation entitled “*Effect of cross-rolling on microstructure, texture and magnetic properties of cold rolled non-oriented electrical steels.*” by “*Jitendra Kumar Mishra*” Roll Number **214MM2501** is a record of original research carried out by him under my supervision and guidance in partial fulfillment of the requirements of the degree of *Master Of Technology* in *Department of Metallurgical and Materials Engineering*. Neither this dissertation nor any part of it has been submitted for any degree or diploma to any institute or university in India or abroad.

.....

Prof. Santosh Kumar Sahoo

DECLARATION OF ORIGINALITY

I, Jitendra Kumar Mishra, roll no. 214MM2501 hereby declare that this dissertation entitled **“Effect of cross-rolling on microstructure, texture and magnetic properties of cold rolled non-oriented electrical steels”**. Represents my original work carried out as a postgraduate student of NIT Rourkela and, to the best of my knowledge, it contains no material previously published or written by another person, nor any material presented for the award of any other degree or diploma of NIT Rourkela or any other institution. Any contribution made to this research by others, with whom I have worked at NIT Rourkela or elsewhere, is explicitly acknowledged in the dissertation. Works of other authors cited in this dissertation have been duly acknowledged under the section "References". I have also submitted my original research records to the scrutiny committee for evaluation of my dissertation.

I am fully aware that in case of any non-compliance detected in future, the Senate of NIT Rourkela may withdraw the degree awarded to me on the basis of the present dissertation.

May26, 2016

NIT Rourkela

Jitendra Kumar Mishra

ACKNOWLEDGEMENTS

This thesis is a result of research that has been carried out at **National Institute of Technology, Rourkela**. During this period, I came across with a great number of people whose contributions in various ways helped my field of research and they deserve special thanks. It is a pleasure to convey my gratitude to all of them.

In the first place, I would like to express my deep sense of gratitude and indebtedness to my supervisors **Prof.Santosh Kumar Sahoo** for his advice, and guidance from early stage of this research and providing me extraordinary experiences throughout the work. Above all, he provided me unflinching encouragement and support in various ways which exceptionally inspire and enrich my growth as a student, a researcher. His involvement with originality has triggered and nourished my intellectual maturity that will help me for a long time to come. I am proud to record that I had opportunity to work with an exceptionally experienced scientist like him.

I am grateful to, and **Prof. S.C. Mishra**, former Head of Department Metallurgical and Materials Engineering, National Institute of Technology, Rourkela, for their kind support and concern regarding my academic requirements.

I want to thank **Mr. Sandeep Kumar Sahni** for helping me throughout my project work.

My parents deserve special mention for their inseparable support and prayers. They are the persons who show me the joy of intellectual pursuit ever since I was a child. I thank them for sincerely bringing up me with care and love.

Place: NIT Rourkela

Date:

Jitendra Kumar Mishra

ABSTRACT

Cross rolled non-oriented (CRNO) electrical steel have uniform magnetic properties in all angular direction. However, controlling the texture for uniform magnetic properties of these steels has been investigated by many researchers. In the present thesis effect of cross-rolling and subsequent annealing of CRNO steels on their texture and magnetic properties have been investigated. Hot rolled non-oriented electrical steel samples were subjected to multi-step cross rolling of 80% reduction in thickness. The rolled samples were then annealed at 650, 750 and 850 °C for 1, 2 and 4hrs respectively. Two different types of samples were used for the present study: one had higher amount of aluminum (sample 1) and another had higher carbon, silicon, manganese, Sulphur and phosphorus content (sample 2). Sample1 had higher grain size as compare to that of sample2 after annealing. Average grain size was increased with increasing the temperature and soaking time of annealing. It was also observed that the various textures (111) <uvw> fiber, (001)<uvw> fiber, (110)<uvw> fiber {110} <100> Goss orientation and {100} <001> cubic orientation which were uniform along different directions of the samples. The magnetic property (in terms of core losses) was found to be lower for samples having higher grain sizes.

Keywords: electrical steel, microstructure, multi-step cross rolling, annealing, texture, core loss.

CONTENT

Certificate of Examination	ii
Supervisor's Certificate	iii
Declaration of Originality	iv
Acknowledgment	v
Abstract	vi
List of Figures	ix
List of Tables	xi
1. INTRODUCTION	1
1.1 Background	2
1.2 Objective	3
1.3 Framework of the thesis	3
2. LITERATURE REVIEW	4
2.1 Electrical steels	5
2.1.1 Factor affecting the Properties of electrical steel.	5
2.1.2 Type of electrical steel	6
2.1.2.1 Grain oriented electrical steel	7
2.1.2.2 Grain non-oriented electrical steel.	7
2.2 Texture	7
2.2.1 Grain orientations	8
2.2.2 Pole figure	9
2.2.3 Euler angle	11
2.2.4 Euler space	12
2.2.5 Orientation distribution function	13
2.3 effect of texture and magnetic properties in electrical steel.	14
3. EXPERIMENTAL DETAILS	16
3.1 Material and Working Procedure	17
3.2 Texture characteristic	17

3.3 Magnetic Properties.	18
4. RESULTS AND DISCUSSION	19
4.1 Results	20
4.1.1 Microstructure and grain size	20
4.1.2 Texture	27
4.1.3 Magnetic properties	38
4.2 Discussion	40
5. CONCLUSION	43
REFERENCES	

LIST OF FIGURES

2.1	manufacturing procedure of electrical steel	5
2.2	Effect of addition of silicon on various properties like % of elongation, crystal isotropy, saturation induction	6
2.3	(a) Preferred texture in material, (b) random texture in material, (c) some orientation is texture and same random	8
2.4	(a) Orientation of grain in polycrystalline material, (b) miller indices and three direction RD, ND, TD in sheet	9
2.5	(a) Projection of plane and reference sphere with a specimen are situated at the center, (b) projection of poles RD, TD and ND on reference plane creating the sample reference frame of a pole figure. (c) The point of intersection of the plane (001), (100) and (010) of the sample on the reference sphere system. (d) Basic circle has projection of three poles 001, 100 and 010. (e) Clustering of estimated poles of (001), (100), and (100) planes from different grains of the sample (f) contour lines represent the pole densities	10
2.6	(a) Orientation of crystal axis system $\{X_i^c\}$ and sample axis system $\{X_i\}$; s is the intersection of planes (RD-TD) and ([100]-[010])	11
2.6	(b) Description of Euler angles φ_1 , φ and φ_2 by Bunge convention in the samples	12
2.6	This diagram demonstrations that how rotation through the Euler angle φ_1 , φ , φ_2 in order to 1, 2, 3 as shown in figure	12
2.7	Graphical demonstration of crystallographic orientations with Euler angle	13
4.1	Microstructure of 1.45% Si CRNO electrical steel annealed at 650 °C for (a) 1 hour (b) 2 hours(c) 4 hours	20
4.2	Microstructure of 1.45% Si CRNO electrical steel annealed at 750 °C for (a) 1 hour (b) 2 hours(c) 4 hours.	21
4.3	Microstructure of 1.45% Si CRNO electrical steel annealed at 850 °C for (a) 1 hour (b) 2 hours(c) 4 hours.	22
4.4	Microstructure of 1.52% Si CRNO electrical steel annealed at 650 °C for (a) 1 hour (b) 2 hours(c) 4 hours	23

4.5	Microstructure of 1.52% Si CRNO electrical steel annealed at 750 °C for (a) 1 hour (b) 2 hours(c) 4 hours.	24
4.6	Microstructure of 1.52% Si CRNO electrical steel annealed at 850 °C for (a) 1 hour (b) 2 hours(c) 4 hours.	25
4.7	Variation of average grain size of (a) 1.45% Si and (b) 1.52% Si CRNO electrical steel with annealing time at different temperature.	27
4.8	$\Phi_{2=45^\circ}$ sectionODFs of 1.45% Si CRNO electrical steel	27
4.9	$\Phi_{2=45^\circ}$ sectionODFs of 1.45% Si CRNO electrical steel annealed at 650 °C for (a) 1 hour (b) 2 hours(c) 4 hours	28
4.10	$\Phi_{2=45^\circ}$ sectionODFs of 1.45% Si CRNO electrical steel annealed at 750 °C for (a) 1 hour (b) 2 hours(c) 4 hours.	29
4.11	$\Phi_{2=45^\circ}$ sectionODFs of 1.45% Si CRNO electrical steel annealed at 850 °C for (a) 1 hour (b) 2 hours(c) 4 hours	30
4.12	$\Phi_{2=45^\circ}$ sectionODFs of 1.52% Si CRNO electrical steel annealed at 650 °C for (a) 1 hour (b) 2 hours(c) 4 hours.	31
4.13	$\Phi_{2=45^\circ}$ sectionODFs of 1.52% Si CRNO electrical steel annealed at 750 °C for (a) 1 hour (b) 2 hours(c) 4 hours.	32
4.14	$\Phi_{2=45^\circ}$ sectionODFs of 1.52% Si CRNO electrical steel annealed at 850 °C for (a) 1 hour (b) 2 hours(c) 4 hours.	33
4.15	variation of volume fraction of (111) $\langle uvw \rangle$ { γ fiber}, (110) $\langle uvw \rangle$ { α fiber}, (100) $\langle uvw \rangle$ { θ fiber}, (100) $\langle 001 \rangle$ {cube orientation},(110) $\langle 001 \rangle$ {Goss orientation} with annealing time annealed at (a) 650°C (b) 750°C (c) 850°C.	36
4.16	variation of volume fraction of (111) $\langle uvw \rangle$ { γ fiber}, (110) $\langle uvw \rangle$ { α fiber}, (100) $\langle uvw \rangle$ { θ fiber}, (100) $\langle 001 \rangle$ {cube orientation},(110) $\langle 001 \rangle$ {Goss orientation} with annealing time annealed at (a) 650°C (b) 750°C (c) 850°C.	38
4.17	Variation core loss (W/kg) with respect to time (hr.) at various temperature (°C) for sample 1 and 2 in figure (a) and (b).	40

LIST OF TABLES

3.1	material confirmation (wt. %) of CRNO electrical steel	17
4.1	Average grain size of sample 1	26
4.2	Average grain size of sample 2	26
4.3	volume fraction of gamma fiber, alpha fiber, theta fiber, cube orientation, Goss orientation at different annealed condition in sample 1	34
4.4	Volume fraction of gamma fiber, alpha fiber, theta fiber, cube orientation, Goss orientation at different annealed condition in sample 2	35
4.5	Core loss at various annealed condition in sample 1	38
4.6	Core loss at various annealed condition in sample 2	39

CHAPTER 1

1. INTRODUCTION

1.1 Background:

Electrical steels are predominantly used as core material for generators, transformers and motors. Two types of electrical steels have been developed: CRGO (cold rolled grain oriented) and CRNO (cold rolled non-oriented) electrical steels. The grain oriented steels typically contain large grains with a typical orientation of $\{110\}\langle 001\rangle$ type Goss orientation and these steels are used in applications involving unidirectional flux paths such as transformer cores. However, non-oriented steels are being used in electrical motors where the flux direction may change or rotate [1, 2].

The magnetic behavior of this material is mainly dependent on two microstructural characteristics: texture and the average grain size [3-5]. Although the chemical composition has also significant effect on the magnetic properties of these steels [3-5]. Various types of textures found in electrical steels are: Goss $\{110\}\langle 100\rangle$, cube $\{100\}\langle 001\rangle$ and eta $\{hkl\}\langle 100\rangle$ [6-7]. (001) $\langle uvw\rangle$ and (111) $\langle uvw\rangle$ fiber have good and bad texture from magnetic point of view [8, 10]. Optimum grain size has to be maintained for minimum core loss in the electrical steels. Average grain sizes of 100 μm and 150 μm for 1.85% and 3.2% Si in steel respectively has been found to be adequate good magnetic property of these steels [11, 12].

Instead of obtaining uniform texture in all directions of the CRNO steels, randomization texture may be more beneficial for obtaining uniform magnetic properties in these steels. Multi-step cross rolling (MSCR) has been proved to be an efficient method for weakening the texture of the material [13-14]. Material is rotated by 90° in each step of rolling process during MSCR [15]. Keeping this in mind the present study was aimed to find out the effect of multi-step cross rolling of the CRNO steels on the texture, microstructure and magnetic properties of these steels.

1.2 Objectives:

The following objectives are planned for the present study:

- i. Effect of cross-rolling on the texture, microstructure and magnetic properties of the CRNO steels.
- ii. Investigation of above (i) for two different compositions of CRNO steels
- iii. Effect of annealing of cross-rolled CRNO steels on their texture, microstructure and magnetic properties
- iv. Correlation of texture, microstructure and magnetic properties of the above (i, ii and iii) processed samples.

1.3 Framework of the Thesis:

Five chapters are discussed in this thesis. Chapter I discusses mainly about the introduction of the project work. Chapter II gives a general outline of electrical steels including the factors important in deciding the electrical properties of these steels, followed by texture of materials and their representation. Subsequently the role of texture in improving the magnetic properties of electrical steels has been discussed based on available literature. Chapter III includes the detailed information about the CRNO steel, the material used in the present study and methods of sample preparation followed by their characterization by different techniques. Chapter IV gives information about the results of the characterizations mainly done for the measurement of the texture and the magnetic properties of the samples and then the discussion of the result obtained. Chapter V concludes the present project work.

CHAPTER 2

2. LITERATURE REVIEW

2.1 *Electrical steels:*

Electrical steel is a soft magnetic material which is manufactured by an optimum amount of Silicon and Carbon mixture. Apart from these certain other metals are added to enhance the property of this steel, like Aluminium, Manganese, etc. Electrical steel sheets are functional materials prepared by adjusting the magnetic behavior of steel for proficient magnetism and electricity translation. It is extensively used in electrical applications such as core material like transformer cores, motor and generator preferably [16]. A flow sheet is shown in Figure 2.1 [17] for the production steps generally adopted in the production of electrical steels.

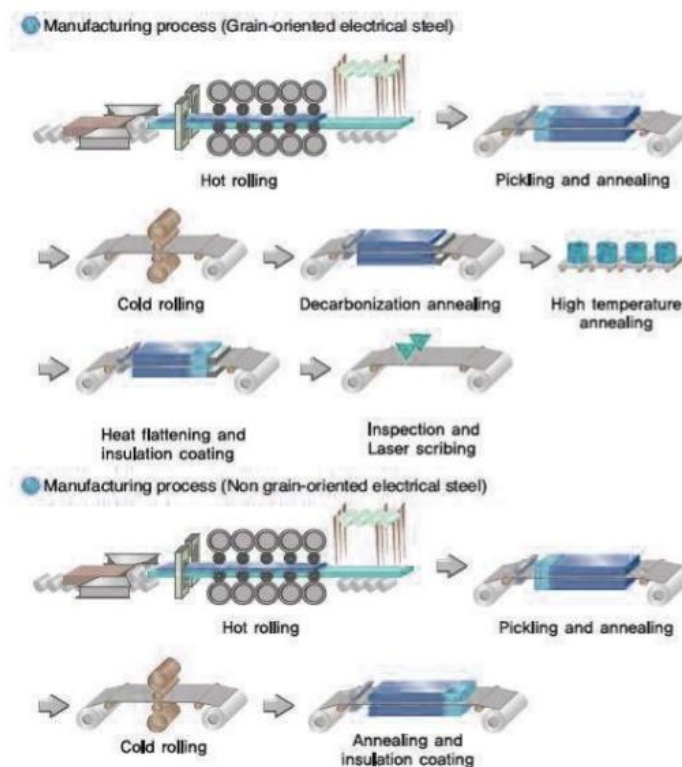


Fig.2.1 manufacturing procedure of electrical steel [17].

2.1.1 *Factor affecting the Properties of electrical steel:*

Electrical steel has three factors: i.e. composition, texture and grain size which are responsible for variation in properties. In electrical steel, silicon increases the resistivity which helps to decrease the eddy current loss. 0 to 6.5% of silicon is used in electrical steel making process but at commercial level, 3.0% of silicon is allowed because if silicon

content is higher than 3%, cold deformability is considerably afflicted and brittleness during cold rolling operation. Al and Mn are allowed up to 0.5% in electrical steel. Al and Mn both act as a growth inhibitors up to 0.5% in electrical steel and if Al and Mn increase more than 0.5% then formation of grain growth is abnormal at lower temperature. Carbon percentage is not exceeded to 0.8 % because beyond this of carbon, ductility of electrical steel decreases [18]. Except (111) $\langle uvw \rangle$ fiber, all fibers improve the magnetic properties and (100) $\langle uvw \rangle$ is the most fiber for electrical steel. Hysteresis loss decreases with increasing magnetic domain size and domain size increases with increasing grain size in electrical steel. When grain size increases in electrical steel then eddy current component of core loss also increases. Permeability is also a factor which effects the material, higher permeability is required in electrical steel because permeability direct affect the core loss of material. Formability of electrical steel should be maintain after thermo-mechanical processing, good formability is required for soft magnetic material.

2.1.2 Type of electrical steels:

- Grain-oriented electrical steel (GO).
- Grain-non-oriented electrical steel (GNO).

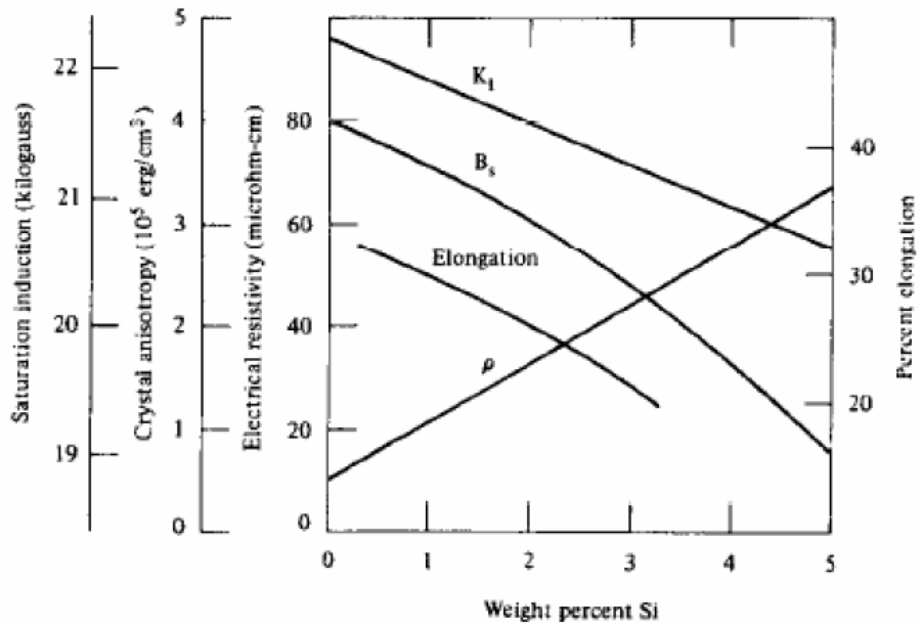


Fig.2.2 Effect of addition of silicon on various properties like % of elongation, crystal isotropy, saturation induction [18]

2.1.2.1 Grain oriented electrical steel:

The term grain oriented is used to appoint electrical steels that possess magnetic properties which are strongly oriented along the rolling direction. Electrical steel having a huge amount of Goss texture (110) [001] are called GO, and it is utilized where unidirectional magnetic flux is required. We know that the magnetization direction whose Goss texture is $\langle 100 \rangle$ is parallel to rolling direction [19]. The Goss texture of GO is controlled to minimize the core loss. Grain-oriented electrical steel is produced at very low level due to its economical factor, but its positive point is its attractive properties e.g., its unidirectional magnetic property and mechanical property. CRGO Grain Oriented Laminations are so huge that good physical nature would be difficult to retain after an 843°C stress relief anneal [20].

2.1.2.2 Non-oriented electrical steel:

GNO are electrical steels in which high amount of Goss texture is absent and its main technological use is the advancement in rotary electrical machinery like stator and rotor which has its magnetic field in the same plane that the sheet has, but the angle connecting the electric field, magnetic field, and rolling direction always alters while performing operation. In non-oriented electrical steel, there is no possibility of magnetization in the direction of $\langle 111 \rangle$ fiber, while the same can be achieved easily in the direction parallel to rolling direction for material, i.e. $\langle 100 \rangle$, and suitable texture would be $\{100\} \langle uvw \rangle$, also called $\langle 100 \rangle$ fiber texture, where most of the grains would have their $\{100\}$ planes parallel to the plane of the sheet [20]. Non-Grain Oriented Electrical steel comprises between 0.5 and 3.25% Si and up to 0.5% Al, added to increase resistivity and lower the temperature of primary recrystallization [21]. For getting the random texture and uniform magnetic properties, we go for annealing operation. Production of non-oriented electrical steel is very high tonnage level today.

2.2 Texture:

If material shows crystallographic texture then it means grains are not randomly distributed. Texture is one of the parameters which affect the magnetic properties [22]. If the material has good texture then it is easily magnetized otherwise if the material has bad texture then magnetization of material faces difficulty. The crystallographic texture could

be illustrated by Orientation Distribution Function (ODF) or Pole Figure (PF). Morphological texture is explained in figure 2.2 [23]. When all possible orientations of the crystallites occur with equivalent frequency, the orientation requirement of properties will disappear due to averaging, and the polycrystalline material can be said isotropic. Complete isotropic characteristics are difficult to achieve, sometimes desirable and sometimes undesirable. All grains are oriented so that the $\{001\}$ planes lie nearly parallel to the plane of the sheet and the $\langle 100 \rangle$ directions point almost in the rolling direction. The texture $\{001\} \langle 100 \rangle$ is highly necessary in substrates for high T_c superconductors [24]. Goss textures $\{110\} \langle 001 \rangle$ are usually preferred in magnetic materials, in which it is easier to magnetize in the cube edge $\langle 100 \rangle$ direction. The texture is easily described by a set of pole figures with the help of X-ray diffraction technique.

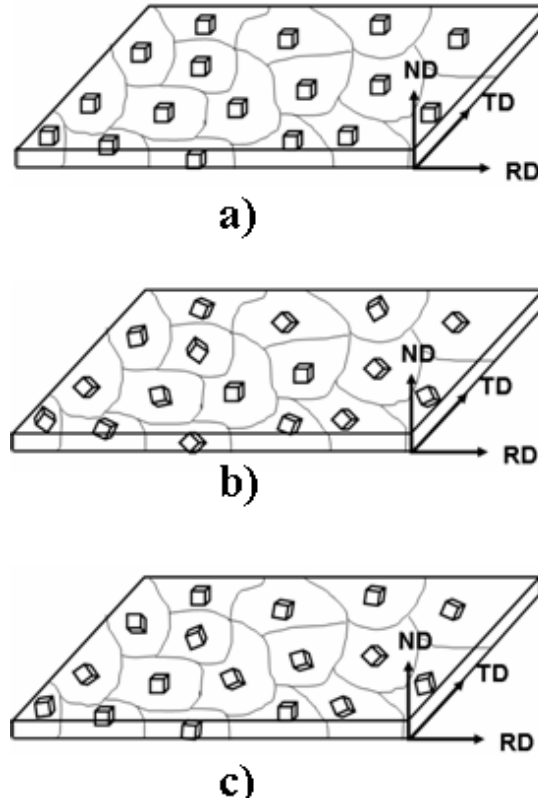


Fig.2.3 (a) preferred texture in material, (b) random texture in material, (c) some orientation is texture and some random [24]

2.2.1 Grain orientation:

The theory of grain orientation is very significant for us because it has the direct relation with Pole figure and Orientation distribution function. The grains' orientation is always represented relative to the coordinate system. The exterior reference plane is

having three directions: (rolling direction (RD), normal direction (ND), and transverse direction (TD)) as in the flat products like a plate or sheet. The grain orientation for a sheet is shown in the below figure 2.3 [18]. Grain orientation is defined by Miller indices which are formulated as $(hkl) [uvw]$. (hkl) Shows the plane and $[uvw]$ shows the direction. It shows that the direction $[uvw]$ is parallel to the rolling direction, and a plane (hkl) is parallel to the rolling plane [25]. Crystal orientation is explained by a set of Miller indices for axisymmetric products like extruded bar and wire which indicates that this crystallographic direction is parallel to the sample axis.

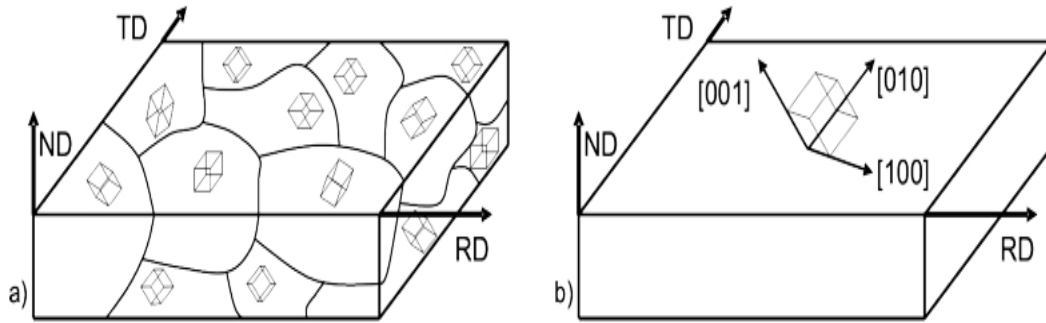


Fig.2.4 : (a) orientation of grain in polycrystalline material, (b) miller indices and three direction RD, ND, TD in sheet [25].

2.2.2 Pole Figure:

The pole figure is the two-dimensional representation of stereographic projection, with crystal orientation defined relative to the specimen geometry, which shows the change of pole density with pole orientation for a chosen set of crystal plane $\{hkl\}$. For analysis the pole figure for rolled sheet of cubic material is explained below: A rectangular portion of sheet material is correlated with three mutually perpendicular specimen parameters perpendicular to the sheet plane, the rolling direction (RD), the transverse direction (TD), and normal direction (ND). When specimen (part of the sample) is too small like point and is placed at the center of the large reference sphere then the following procedure is performed for drawing stereographic projection, where ND is situated at center and TD and RD are on the periphery of the sphere [26]. The three mutually perpendicular planes (100), (010), and (001) of a rectangular specimen are considered to be in the sphere as shown in the figure 2.4(c), which are perpendicular to each other. Points 100, 010, and 111 in figure are poles of planes with these three set of Miller

indices, and these poles on a projection plane are parallel to the surface of the sample as shown in the figure 2.4(d). If projected poles are clustered together, it means that material is textured and if the projected poles are distributed uniformly, that means the material is texture less or random as shown in figure 2.4(e). Pole densities are represented by contour lines as shown in figure 2.4(f)

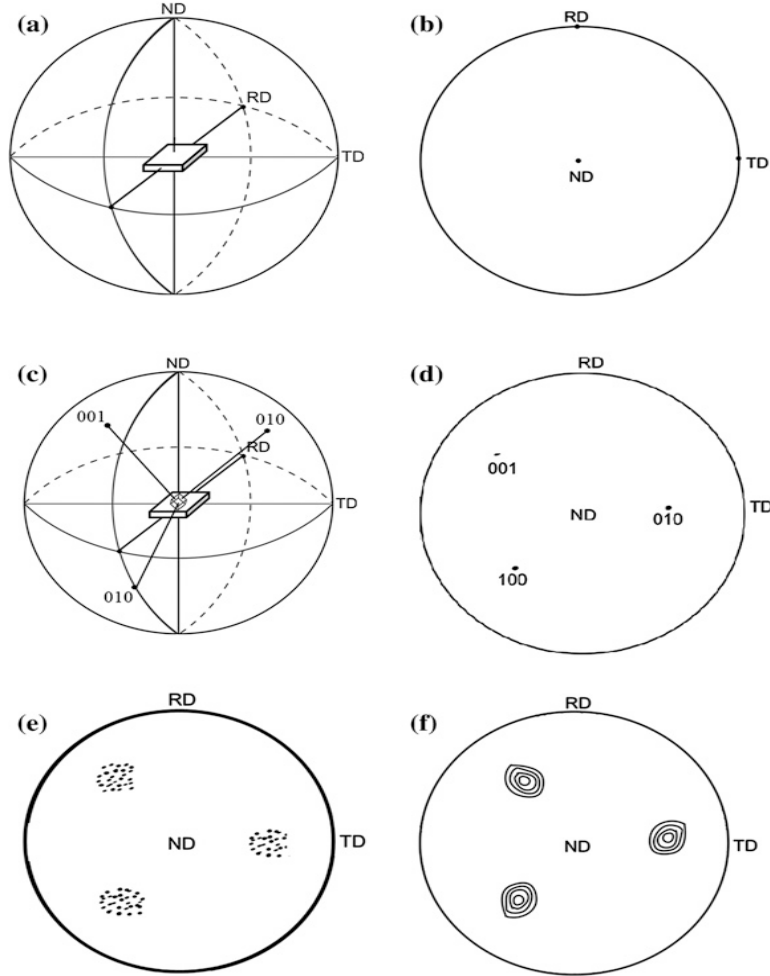


Fig.2.5 (a) Projection of plane and reference sphere with a specimen are situated at the center, (b) projection of poles RD, TD and ND on reference plane creating the sample reference frame of a pole figure. (c) The point of intersection of the plane (001), (100) and (010) of the sample on the reference sphere system. (d) Basic circle has projection of three poles 001, 100 and 010. (e) Clustering of estimated poles of (001), (100), and (010) planes from different grains of the sample (f) contour lines represent the pole densities [27].

2.2.3 Euler Angle:

For the graphical demonstration of an ODF, a technique must be determined to characterize the ‘g’ orientation of grain, where ‘g’ being the parameter of grain orientation. It is determined with the help of Euler angle. Euler angle associates to three rotations when performed in the exact order, the transformation of the coordinate system of sample onto that of the crystal co-ordinate system. For explaining this concept (Euler angle), there are requirements of two different co-ordinate systems, first one is of the sample (sample axes system, X_I) and the other one is of the crystal of grain (crystal axes system, X_i^c). Both of them are following Cartesian coordinate system & right-hand rule (figure: 2.5 (a)) [28]. To take an example of rolled product (sheet), X_1 is represented by RD, X_2 by TD, and X_3 is related to ND of that rolled product (sheet). This rotation of the system should make both systems to overlap each other. The process to achieve this overlap is as explained: The first rotation φ_1 around ND is taken. This takes RD in the location s, where s is the meeting of planes (RD-TD) and the new location of RD and ND are now RD' and ND'. Now, Rotation φ around RD' is carried out which takes ND together with RD'. TD will now move to the location TD''. And lastly, rotation φ_2 around ND is done and due to this rotation, RD' lies on RD_s and TD' shifts to ND_s. Bunge convention is applied for the nomenclature of the rotation angle [5].

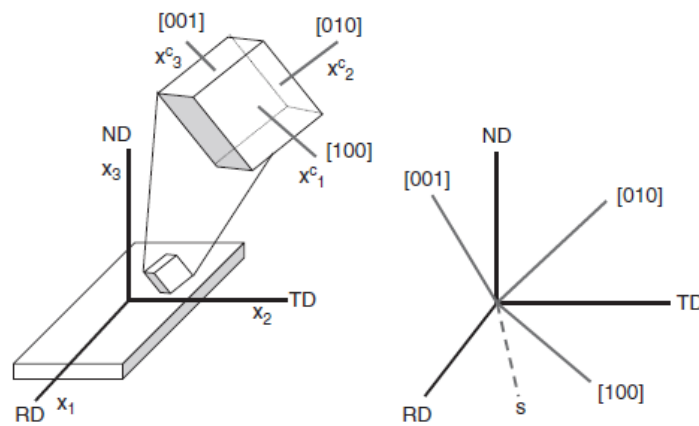


Fig.2.6 (a) orientation of crystal axis system $\{X_i^c\}$ and sample axis system $\{X_i\}$; s is the intersection of planes (RD-TD) and ([100]-[010]). [28]

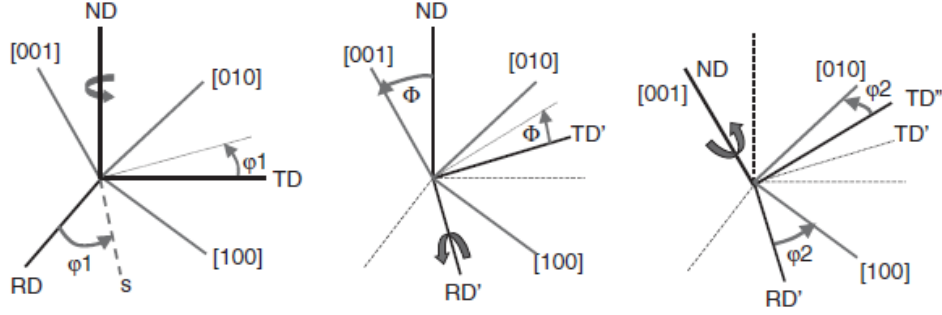


Fig. 2.6(b) description of Euler angles φ_1 , φ and φ_2 by Bunge convention in the samples [29].

- The first rotation φ_1 around ND is taken; this takes RD in the location s, where s is the meeting of planes (RD-TD) and ([100]-[010]). The new locations of RD and ND are now RD' and ND'.
- Rotation φ around RD'; this takes ND together with [001]; TD will move to the location TD'.
- A rotation φ_2 around ND (which is now equal to [001]); due to this rotation, RD' lies on [100] and TD'' shifts to [010].

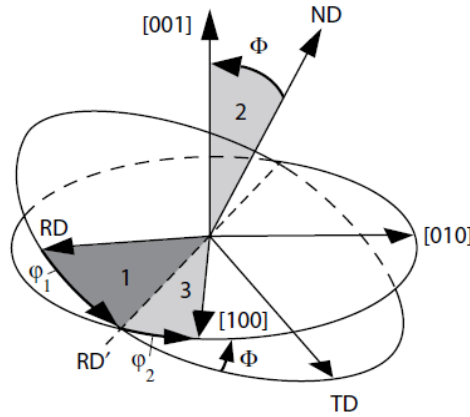


Fig. 2.6. (c): this diagram demonstrates that how rotation through the Euler angle φ_1 , φ , φ_2 in order to 1, 2, 3 as shown in figure [5].

2.2.4. Euler Space:

Every orientation in space is represented with the help of three Euler angles or two Euler angles and keeping the other one constant. Three Euler angle system is used in large sphere, referred in Pole Figure subsection, but it cannot be used for analysis of texture data. Two Euler angle system is used for 2D representation of texture data, keeping the other Euler angle constant and it is normally used in real condition. Euler angles are

plotted in Cartesian coordinate system and separating space among them is called as Euler space. This space is limited for φ_1 and φ_2 between 0° and 360° and Φ is varied from 0° to 180° (fig.) [5].

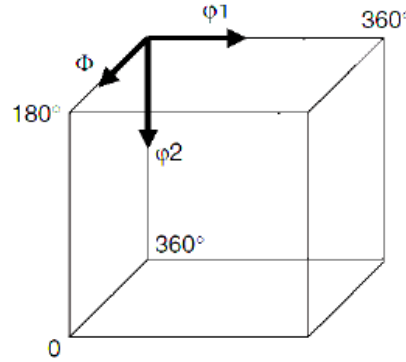


Fig. 2.7: graphical demonstration of crystallographic orientations with Euler angle [7].

2.2.5 Orientation Distribution Function:

Pole figure provides limited information due to its 3-D representation. Because of this, we study texture through orientation distribution function (ODF) which is plotted in a 2-D manner. The ODF method is based on explaining a crystal arrangement in a process which is entirely changed from the general explanation of a direction in the form $\{hkl\}$ $\langle uvw \rangle$. The ODF is a mathematical function that relates the time of appearance of particular crystal orientations in a 3-D Euler space whose coordinates are determined by three Euler angles. These angles result from three consecutive rotations which are required to be given to every crystallite in the specimen, in order to produce its crystallographic axes to coincide with the specimen axes. The complete classification of orientation will then consist of the sets of rotations described to all the crystallites in the specimen. Several mathematical formulations have been structured which permit a mathematical function to be resolute from the numerical data collected from PF's that could explain the orientation of all the crystallites in a polycrystalline material collectively in a more appropriate manner. Such procedures have been proposed independently by Bunge [30], Roe [31]. There are two principal techniques for reconstructing an orientation distribution function based on PF data: (i) harmonic technique which fits the coefficients of spherical harmonic functions to the data, and (ii) discrete technique which calculates orientation distribution

directly in separate representation via an iterative process. If the grain orientation is denoted by a parameter ‘g’, then the expression of ODF series is given below:

$$\frac{dV}{V} = f(g)d(g) \quad (1)$$

2.3 Effect of texture on magnetic properties of Electrical Steels

Magnetic properties are controlled by cross rolling operation because cross rolling directly affects the textural component. Thermomechanical process is required to control the properties of materials which include hot rolling, cross rolling and annealing [7, 18, and 28]. Non-oriented electrical steels are generally used in smaller electrical machines like rotor and stator, requires low and high permeability to provide low core loss. Core loss are basically of two types, hysteresis loss and eddy current loss. Eddy current loss is associated to resistivity and can be controlled by the composition of the material but the hysteresis loss depends on the magnetic anisotropy, which depends on the orientation or texture of the material and can be improved during the treating of the material [32]. Cross-cold rolling changes the initial hot-rolling texture components and produces a strong $\{001\}\langle 110 \rangle$ component. The texture data were correlated to the magnetic properties, and found that, hysteresis loss was 80 % of the total loss and it was due to texture and grain size [32].

Mainly, seven type of texture components are found in cubic materials (non-oriented electrical steel), cube $\{100\}\langle 001 \rangle$, rotated cube $\{110\}\langle 110 \rangle$, Goss $\{110\}\langle 100 \rangle$, theta $\{100\}\langle uvw \rangle$, $\langle uvw \rangle$ and alpha $\{hkl\}\langle 110 \rangle$, eta $\{hkl\}\langle 100 \rangle$, gamma $\{111\}$ [24, 33]. To compare with seven texture, cube texture is most favorable because $\{100\}$ planes have many numbers of $\langle 100 \rangle$ axes which can be easily magnetized. On the other hand, texture with $\{111\}$ planes does not contain $\langle 100 \rangle$ axes and texture with $\{112\}$ planes including $\langle 111 \rangle$ axes are undesirable and should not be utilized for non-oriented electrical steel. The final texture is influenced by all processing steps which are used in the investigation like, hot rolling, hot band annealing, cross rolling (below the recrystallization temperature), recrystallization annealing. The texture with low intensity of $\{112\}\langle 111 \rangle$ and $\{110\}\langle 001 \rangle$ are obtained in hot rolling, meaning that this type of textures are formed at above recrystallization [34]. Low core loss and magnetic induction are obtained in effective manner by using hot band annealing with high temperature. The increase in

planar anisotropy by hot-band annealing can be closely associated to decrease in the $\{211\}$ and $\{222\}$ components and an increase in the $\{110\}$ component. Recrystallization of texture is a very important phase because new strain free grain is introduced in the region from the strained lattice. Gamma fiber $\{111\} \langle uvw \rangle$, Goss $\{110\} \langle 100 \rangle$ and cube $\{100\} \langle 001 \rangle$ components decrease during annealing operation by recrystallization [35].

CHAPTER: 3

3.EXPERIMENTAL DETAILS

3.1 Material and Working Procedure:

2.3 mm thick sheets of materials, chemical compositions as shown in table 3.1, were used for the present investigation. Two different samples were used for the investigation. Sample 1 had the higher amount of aluminum as compared to sample 2 whereas sample 2 had the high amount of carbon, silicon, phosphorous and manganese. Rolling was done to reduce the thickness of samples up to 0.5 mm by multi-step cross rolling in the laboratory rolling mill. Throughout each pass of the samples, the true strain was preserved 10%. After MSCR operation, samples were taken to perform an annealing operation at 650°C, 750°C, and 850°C for 1hr, 2hrs, and 4hrs respectively in tubular furnace. During annealing operation, argon gas was used to create inert atmosphere, and heat rate was maintained at 15°C/minute. Standard operations were followed to polish the samples for the visualization of microstructure. Etching was done prior to microstructure visualization through optical microscope and nital solution was used for etching the samples. Average grain size was measured by Axiovision release 4.8.2 Software. This is an image processing software by which study of high resolution microstructure can be done.

Table 1 material confirmation (wt. %) of CRNO electrical steel.

	C%	Si%	Mn%	P%	S%	Cr%	Ni%	Mo%	Al%	Cu%
Sample1	0.0376	1.45	0.305	0.0201	0.018	0.007	0.0097	0.0021	0.0965	0.0120
Sample2	0.039	1.52	0.35	0.0216	0.020	0	0	0	0.0525	0

3.2 Texture characteristic:

Bruker D8 advance system was used for the characterization of bulk texture. Three different types of pole figure (110), (200), and (211) were dignified which had normal plane with rolling direction and transverse direction. (110), (200) and (211) planes were interacted on the sphere in pole figure. These three points 110, 200 and 211 are referred to as set of miller indices. These projected planes are clustered tougher and formed contour

due to pole intensities. ODFs were estimated using an academic software Labotex 3.0 [36]. Using this software, volume fraction was measured at different-different angles. In present study, value of φ_2 was kept at a constant value of 45° while φ_1 was varied from 0° to 360° and φ was varied from 0° to 360° .

3.3 Magnetic Properties:

Magnetic property (core loss) was measured by Brockhaus MPG 200 machine [37]. Core loss depends on both composition of a material and annealing condition. When magnetic properties increase, cost of production increases in similar way, and that is why we maintain optimum condition for manufacturing.

CHAPTER: 4

4.RESULTS AND DISCUSSION

4.1 RESULT:

4.1.1. Microstructure and grain size:

Microstructure of sample 1, which have 1.45% Si content, annealed at 650 °C for (a) 1 hour (b) 2 hour (c) 4 hour are shown in figure 4.1. It may be observed from the figure 4.1 with increase in soaking time of annealing the grain size was increased.

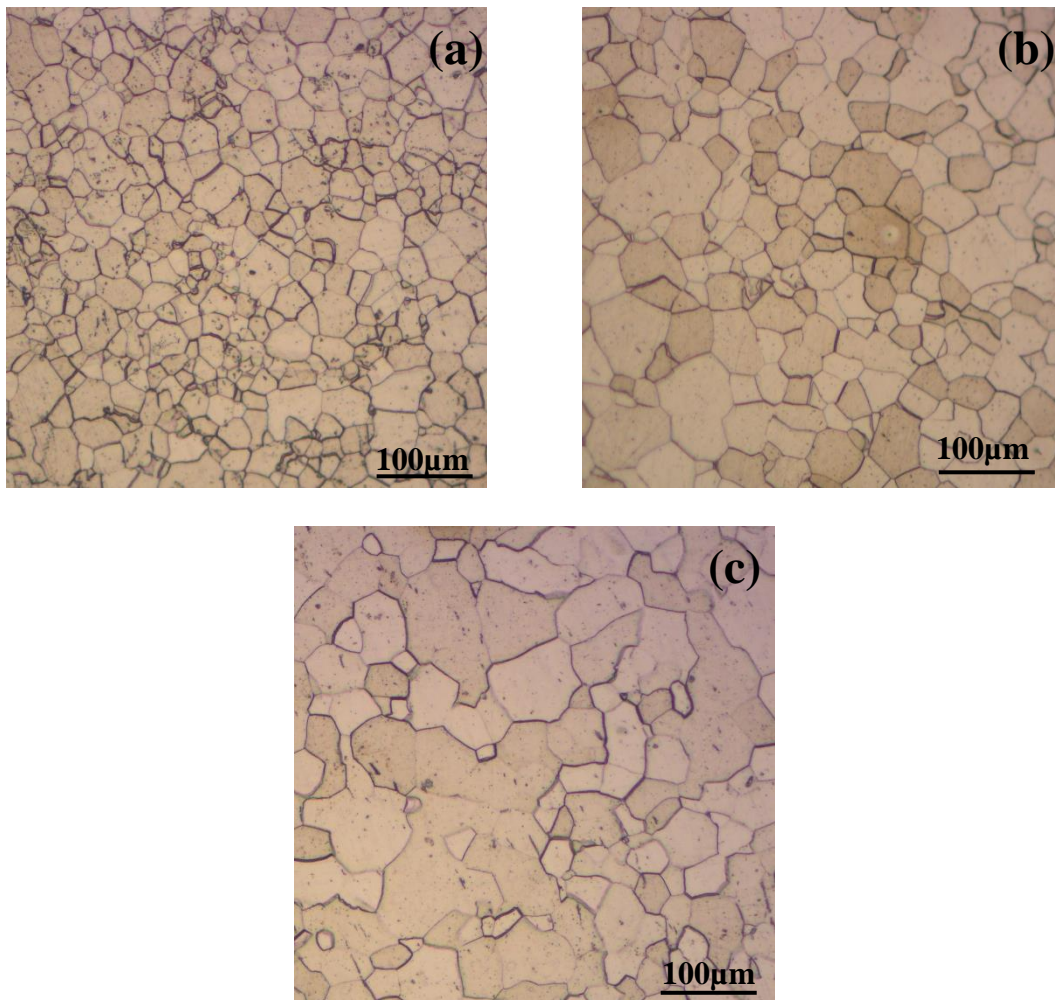


Figure 4.1 microstructure of 1.45% Si CRNO electrical steel annealed at 650 °C for (a) 1 hour (b) 2 hours(c) 4 hours.

Figure 4.2 represents the microstructures of 1.45% Si CRNO electrical steel (sample 1) which were annealed at 750°C for (a) 1 hour, (b) 2 hours, and (c) 4 hour. This condition had coarse grains as compared to previous conditions of annealing (i.e. 650 °C). Also abnormal grain growth of the sample was observed at 4 hrs of annealing time.

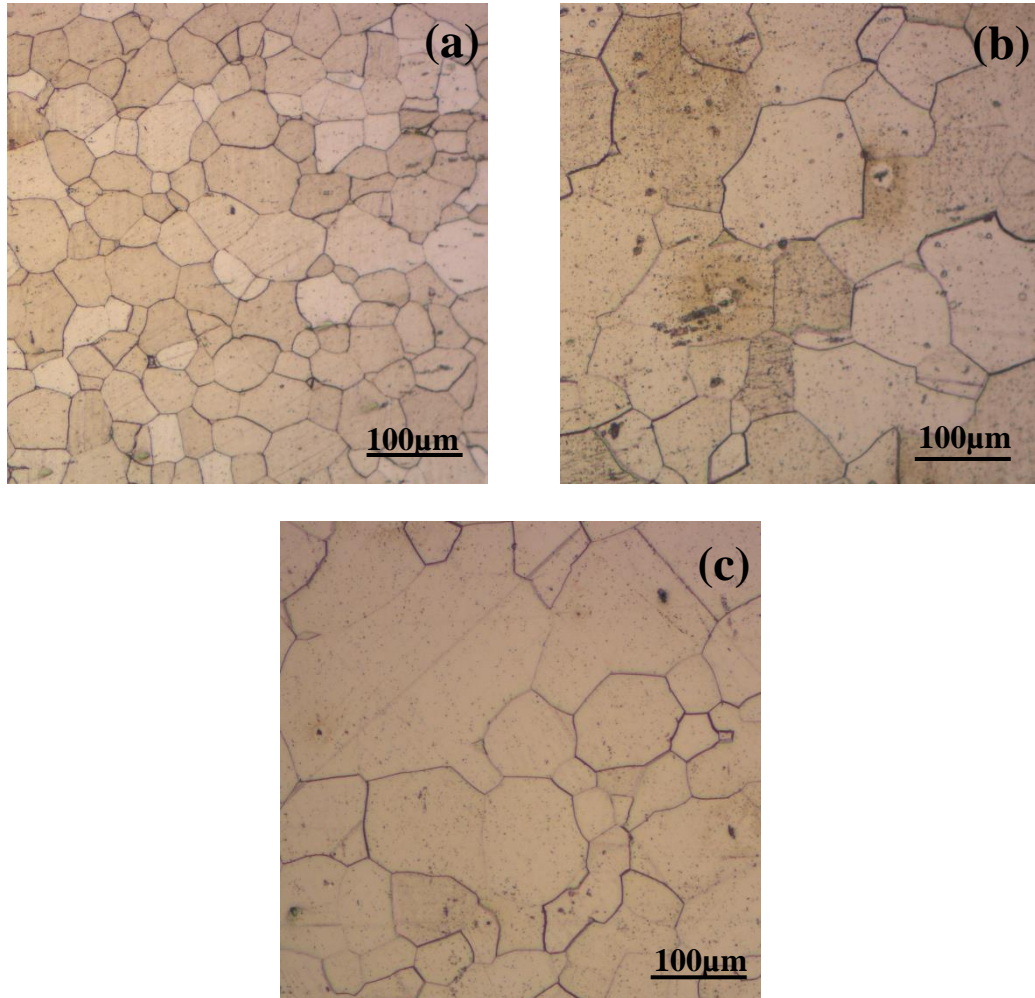


Figure 4.2 microstructure of 1.45% Si CRNO electrical steel annealed at 750 °C for (a) 1 hour (b) 2 hours(c) 4 hours.

Figure 4.3 represents microstructure of sample 1 which contains 1.45% Si annealed at 850°C for (a) 1 hour, (b) 2 hours, and (c) 4 hours. In these conditions, the grain size was observed to be higher than that of previous conditions of annealing. The abnormality of grain growth was also observed in this condition of annealing.

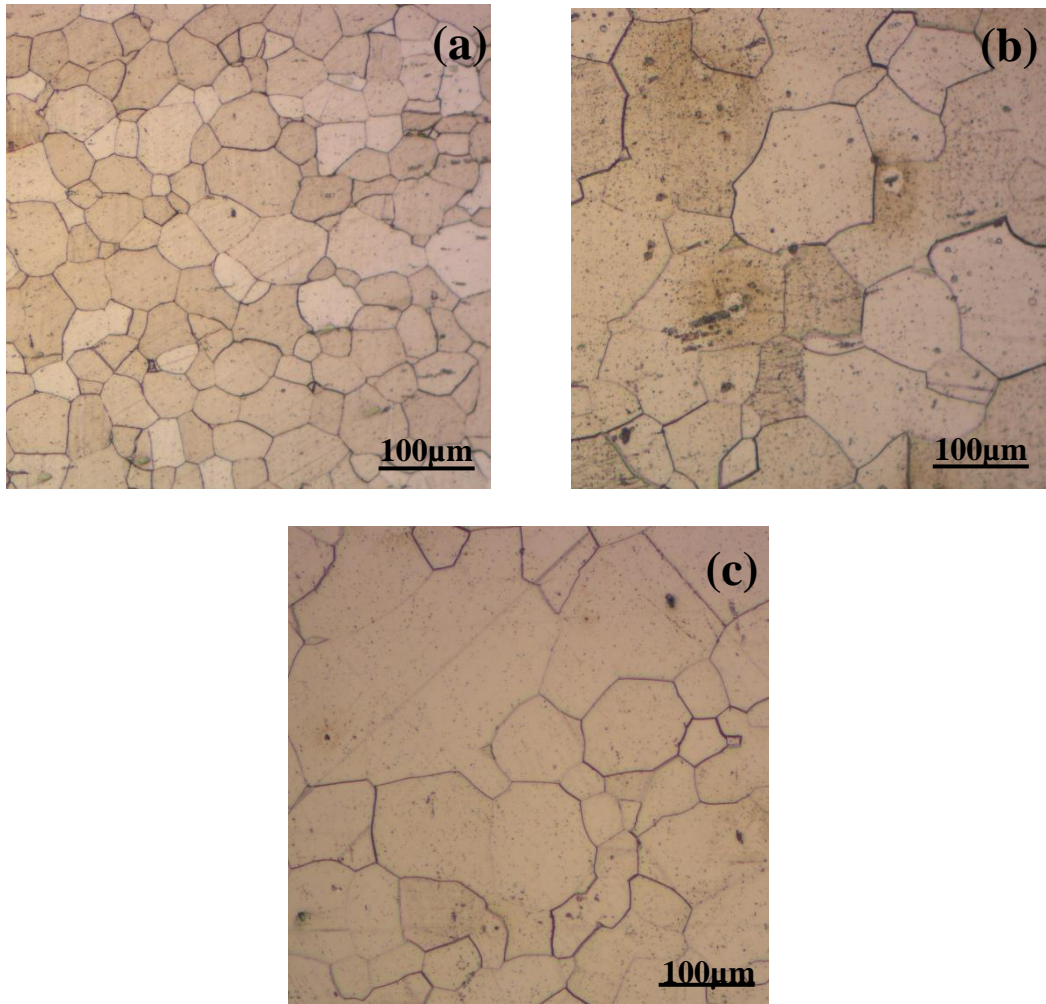


Figure 4.3 microstructure of 1.45% Si CRNO electrical steel annealed at 850 °C for (a) 1 hour (b) 2 hours(c) 4 hours.

Figure 4.4 represents microstructure of sample 2 which contains 1.52% Si annealed at 650°C for (a) 1 hour, (b) 2 hours, and (c) 4 hours. Figure indicates that the grain size increased with increasing the soaking time of annealing of the samples.

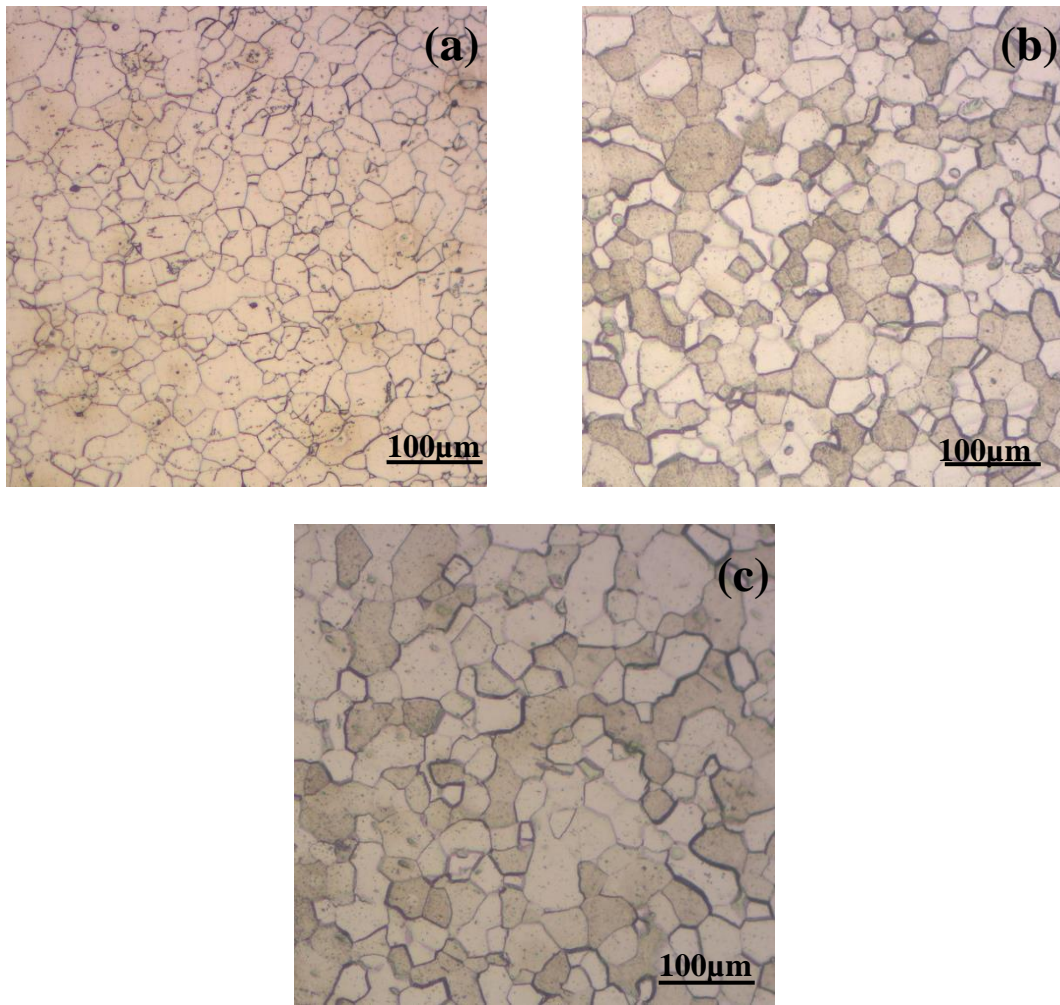


Figure 4.4 microstructure of 1.52% Si CRNO electrical steel annealed at 650 °C for (a) 1 hour (b) 2 hours(c) 4 hours.

Microstructure of sample 2 which has 1.52% Si content annealed at 750°C for (a) 1 hour, (b) 2 hours, and (c) 4 hours are shown in figure 4.5. An insignificant increase in grain size with increase in soaking time of annealing was observed.

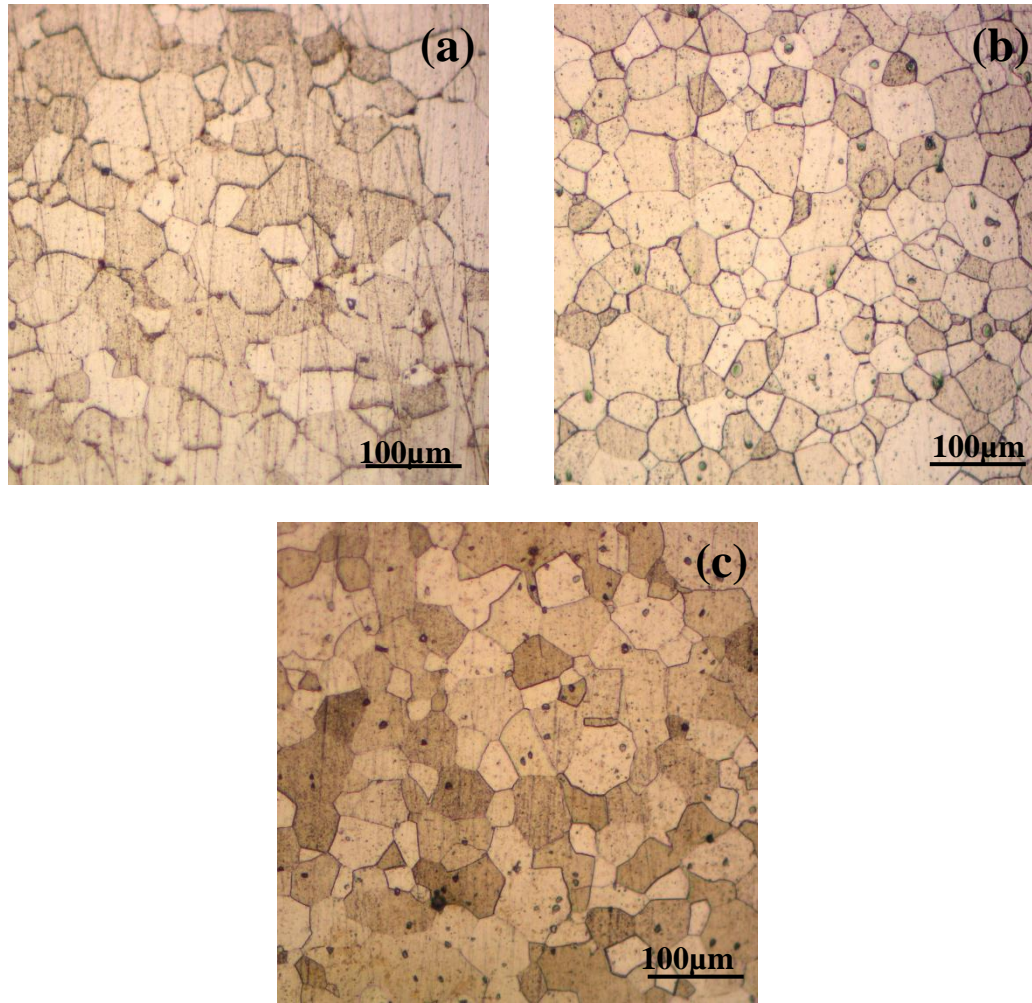


Fig. 4.5: microstructure of 1.52% Si CRNO electrical steel annealed at 750 °C for (a) 1 hour (b) 2 hours(c) 4 hours.

Microstructure of sample 2 which has 1.52% Si annealed at 850°C for (a) 1 hour, (b) 2 hours, and (c) 4 hours as shown in figure 4.6. It indicates that grain size was higher than that of the above annealing conditions.

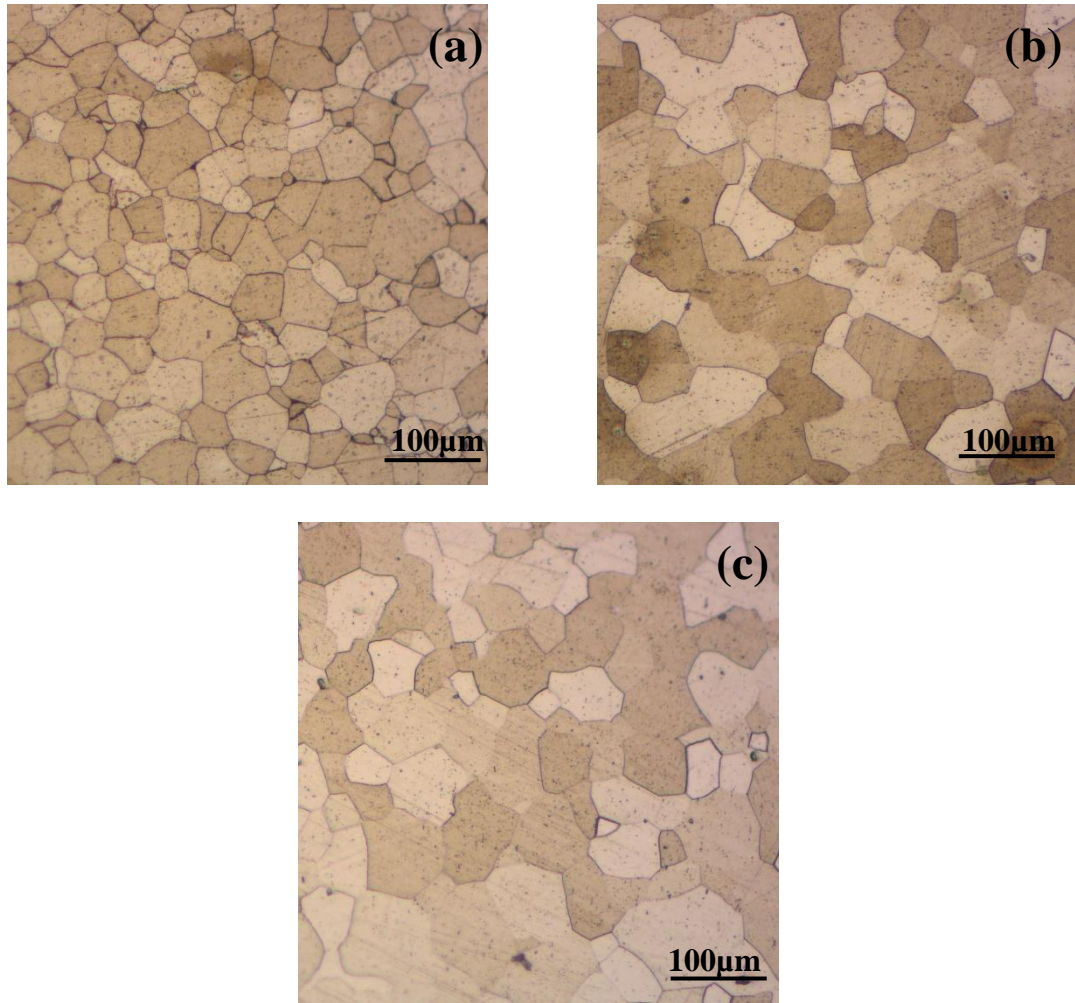


Figure 4.6 microstructure of 1.52% Si CRNO electrical steel annealed at 850 °C for (a) 1 hour (b) 2 hours (c) 4 hours.

Formation of equiaxed grains were observed in both samples. Grain size was dependent on temperature and time. Normal grain growth took place at 650°C for less duration (1 hr and 2 hrs) in sample 1 but when the soaking time was increased to 4 hours, the abnormal grain growth was observed. However, the normal grain growth was observed in the sample 2 during different conditions of annealing. Average grain size of sample 1 and sample 2 are shown in figure 4.7(a) and 4.7(b) respectively and reading of average grain size are given in table no 4.1 and 4.2 respectively. From figure 4.7 (a) and 4.7 (b), it was observed that the average grain size increased with increasing the time and temperature of annealing.

Table 4.1: Average grain size (in μm) of sample 1 at different conditions of annealing.

	650°C	750°C	850°C
1hr	24.87	34.84	39.84
2hrs	26.95	36.04	65.47
4hrs	39.27	47.85	73.46

Table 4.2: Average grain size (in μm) of sample 2 at different conditions of annealing.

	650°C	750°C	850°C
1hr	23.23	36.2	37.89
2hrs	28.03	36.96	41.19
4hrs	28.202	39.32	45.97

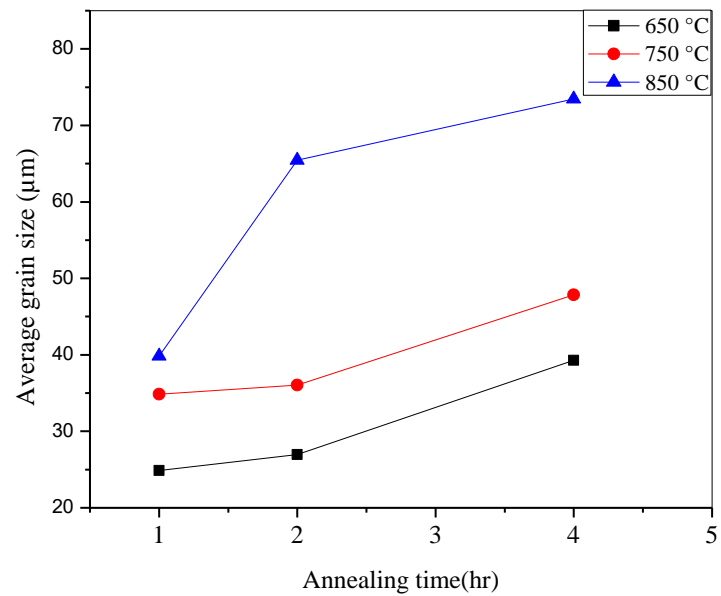


Fig. 4.7(a)

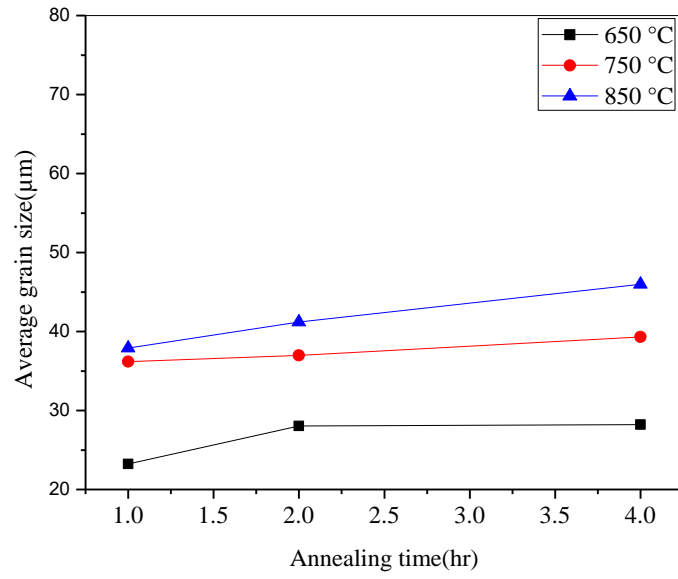


Fig.4.7 (b)

Fig.4.7: variation of average grain size of (a) 1.45% Si and (b) 1.52% Si CRNO electrical steel with annealing time at different temperature.

4.1.2 TEXTURE:

Orientation distribution function (ODF) of sample1 and sample 2 are given in figure 4.8 to figure 4.14, where ϕ_2 is kept constant at 45° . Texture formation in contour form are shown in these figures.

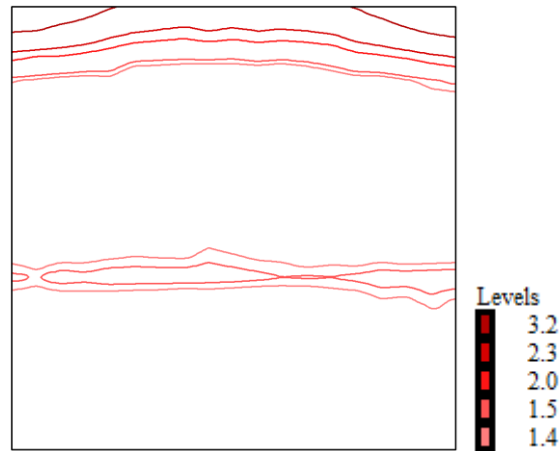


Fig.4.8: $\phi_2=45^\circ$ section ODFs of 1.45% Si CRNO electrical steel (before annealing).

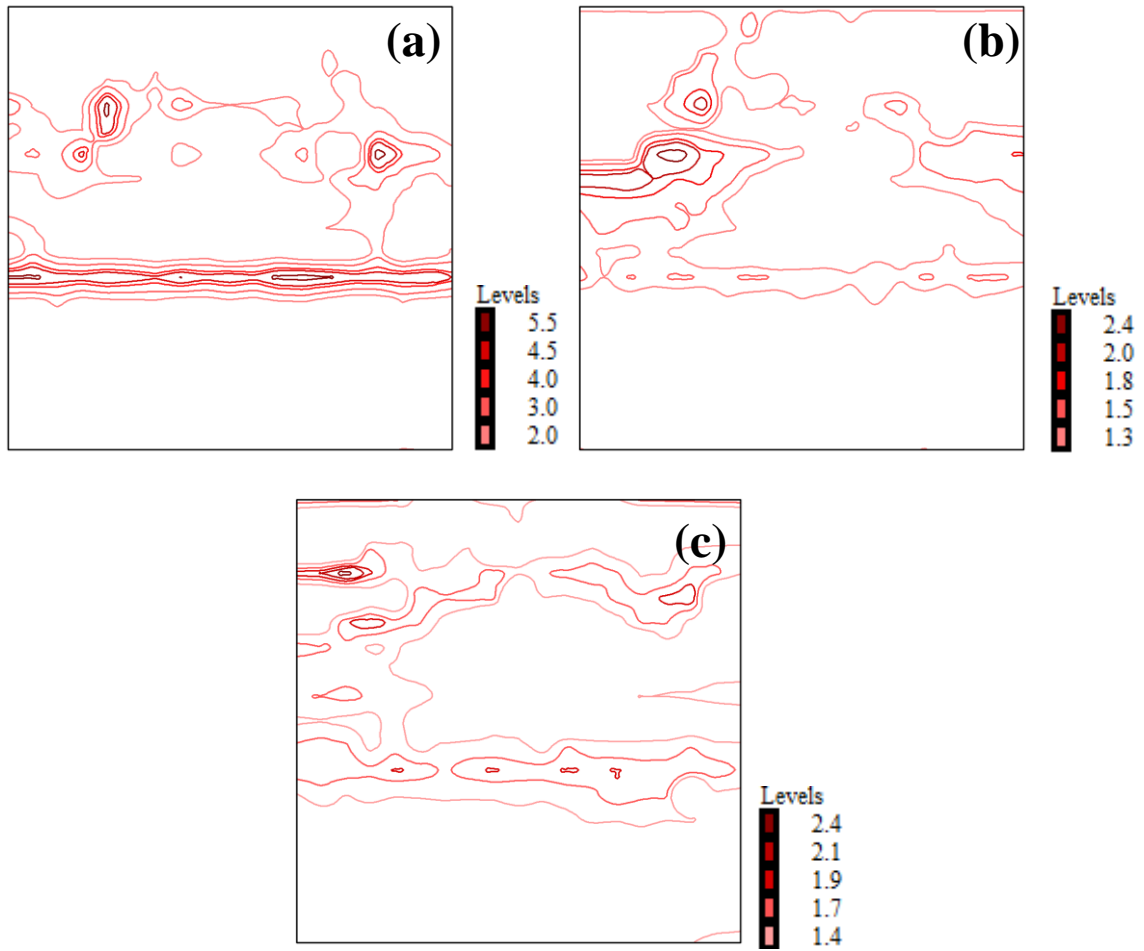


Fig.4.9: $\phi_2=45^\circ$ section ODFs of 1.45% Si CRNO electrical steel annealed at 650 °C for (a) 1 hour (b) 2 hours(c) 4 hours.

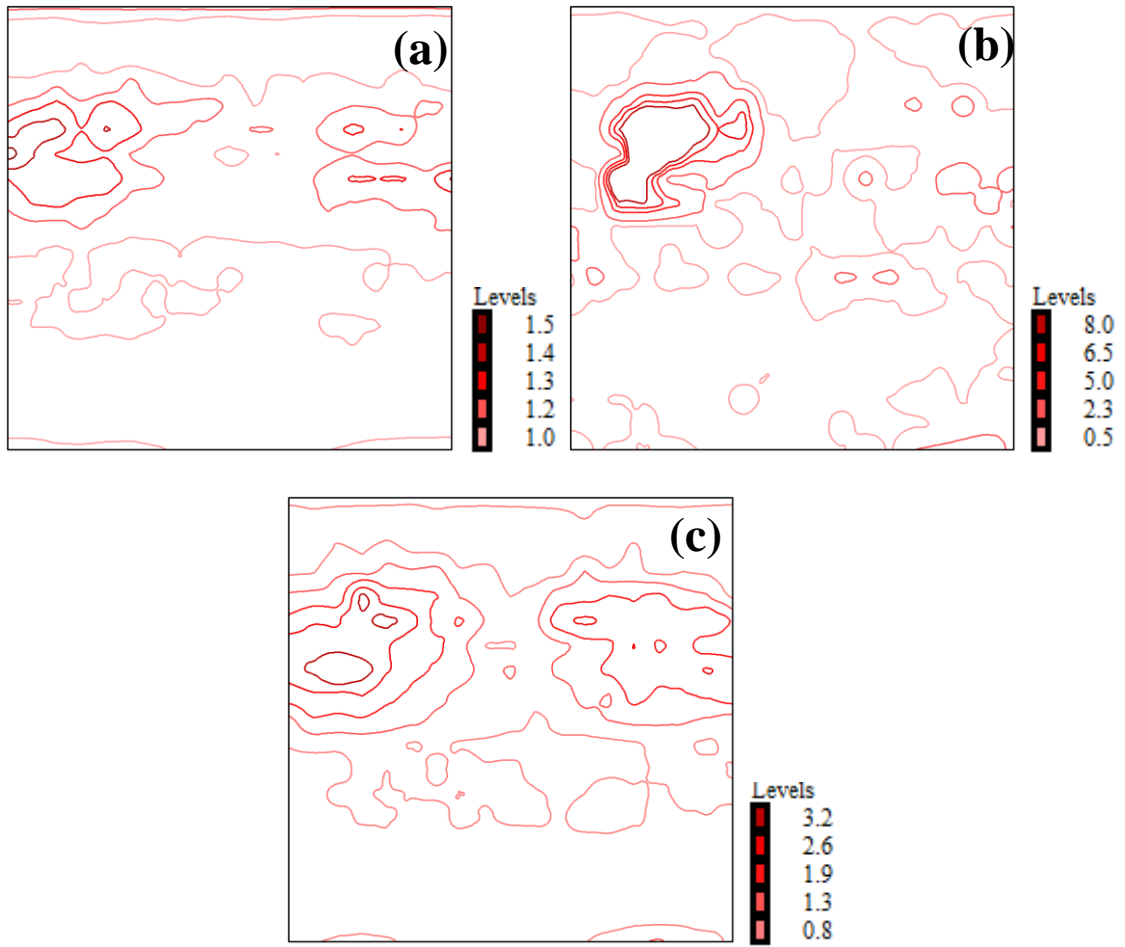


Fig.4.10: $\phi_2=45^\circ$ section ODFs of 1.45% Si CRNO electrical steel annealed at 750 °C for (a) 1 hour (b) 2 hours (c) 4 hours.

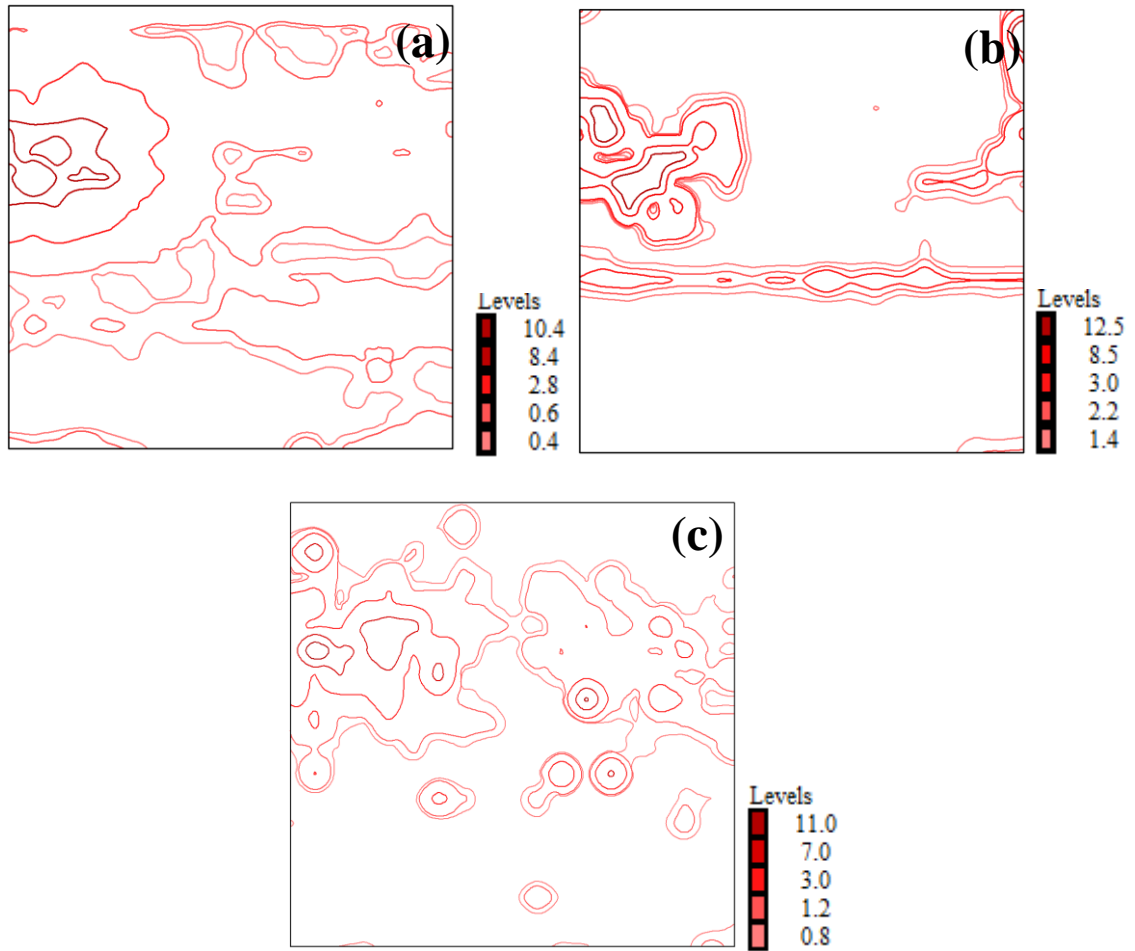


Fig.4.11: $\varphi_2=45^\circ$ section ODFs of 1.45% Si CRNO electrical steel annealed at 850 °C for (a) 1 hour (b) 2 hours(c) 4 hours

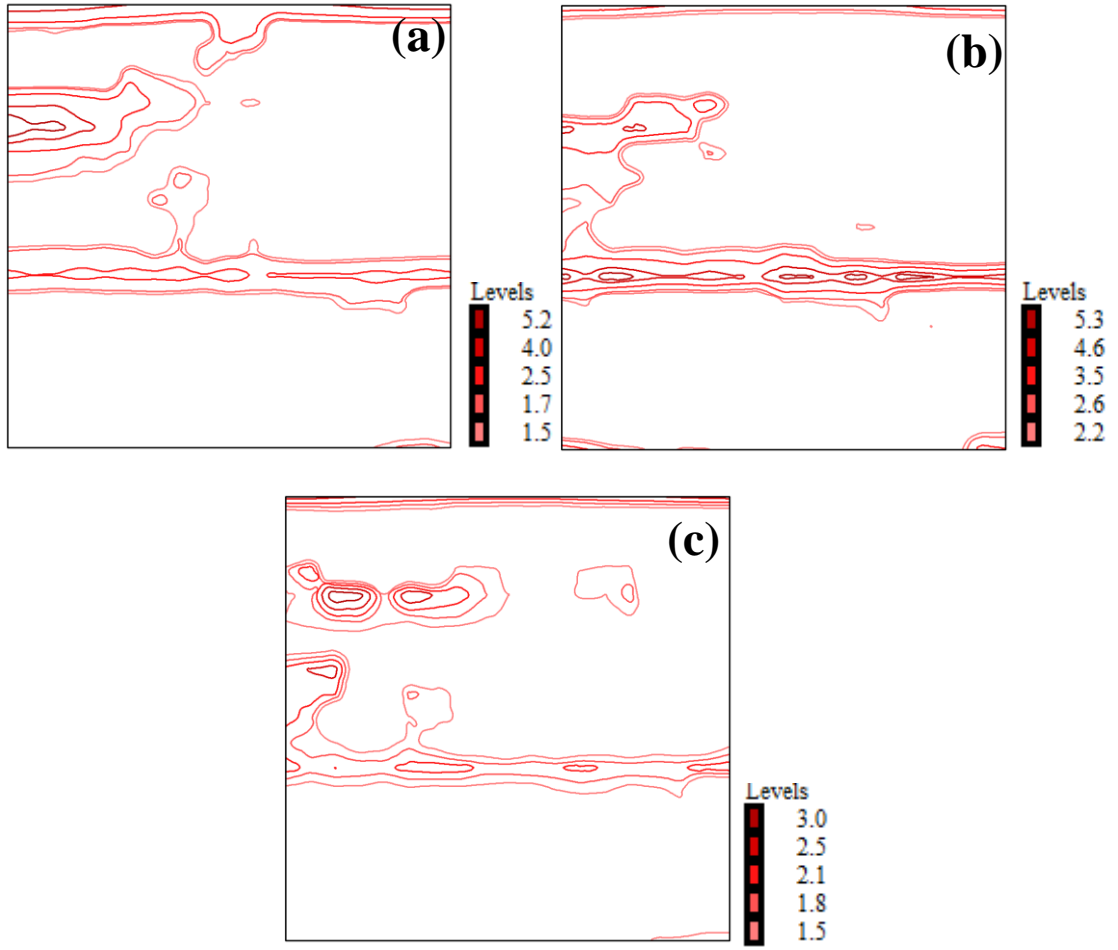


Fig. 4.12: $\phi_2=45^\circ$ section ODFs of 1.52% Si CRNO electrical steel annealed at 650 °C for (a) 1 hour (b) 2 hours (c) 4 hours.

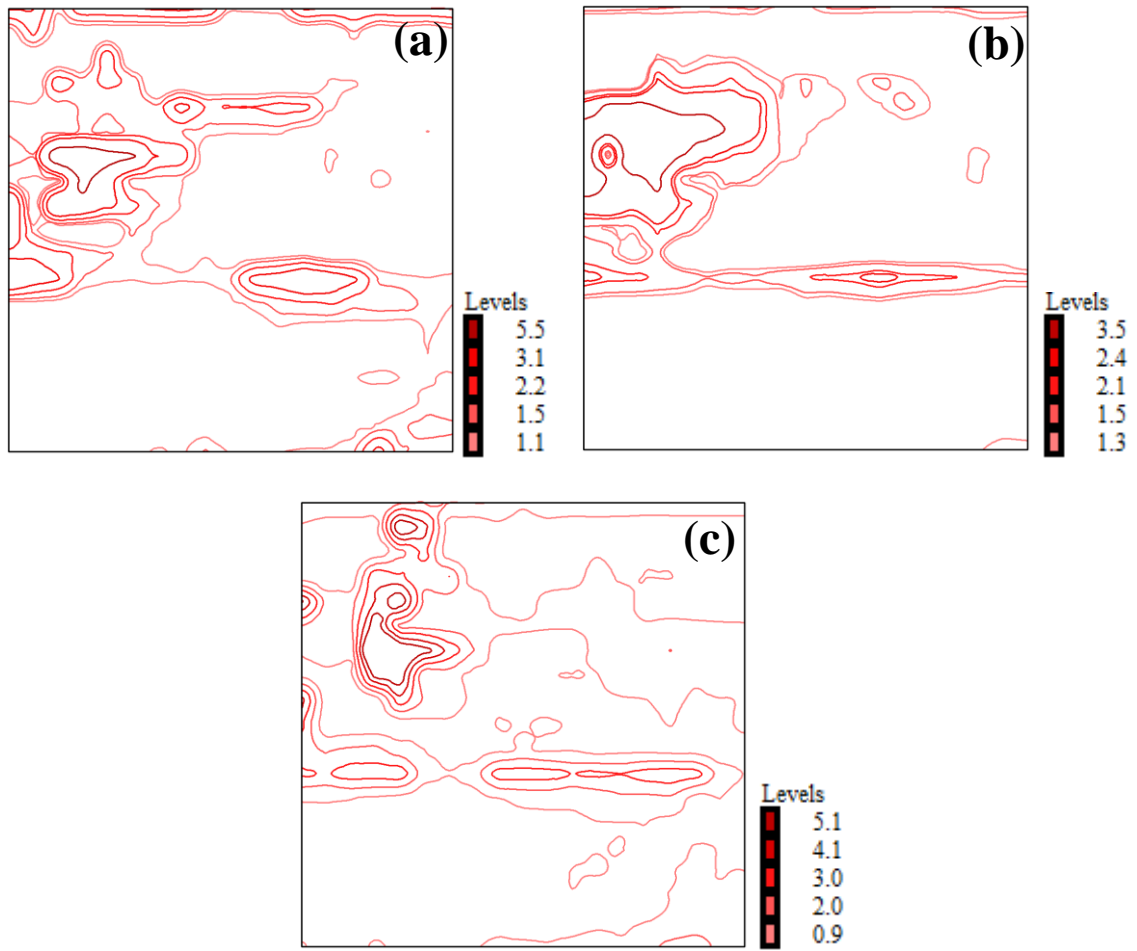


Fig. 4.13: $\phi_2=45^\circ$ section ODFs of 1.52% Si CRNO electrical steel annealed at 750 °C for (a) 1 hour (b) 2 hours(c) 4 hours.

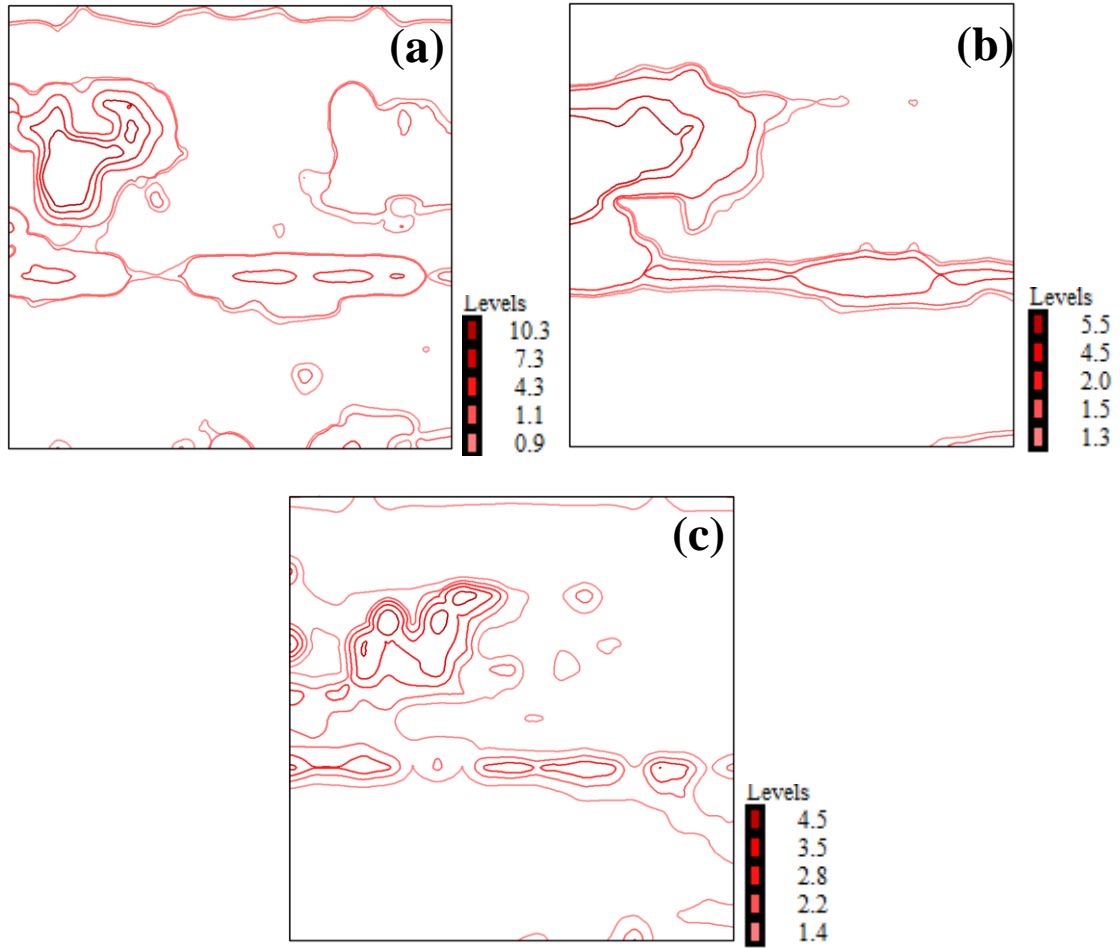


Fig. 4.14: $\phi_2=45^\circ$ section ODFs of 1.52% Si CRNO electrical steel annealed at 850 °C for (a) 1 hour (b) 2 hours (c) 4 hours.

The volume fraction of sample 1 and sample 2 are shown in figure 4.15 and figure 4.16 and volume fractions are given in tabular form in table no 4.3 and 4.4 at different temperature and time. It has come to notice that at different annealing conditions the γ -fiber was distinct. The figure shows that volume fraction (VF) of (111) $\langle uvw \rangle$ fiber decreases at 650°C in sample 1 and increases in sample 2 during 1hr to 2hrs. At same condition, volume fraction of (110) fiber is increasing in sample 1, little higher than volume fraction of (111) $\langle uvw \rangle$ fiber and volume fraction of (110) $\langle uvw \rangle$ fiber is also increasing in sample 2 but less than volume fraction of (111) $\langle uvw \rangle$ fiber. At 650°C and 4hrs, (111) $\langle uvw \rangle$ fiber and (110) $\langle uvw \rangle$ fiber are almost same in sample 1 and sample 2 but VF is different for both samples. VF of (110) $\langle uvw \rangle$ fiber is higher at 750°C in sample 1 and VF of (110) $\langle uvw \rangle$ fiber is also higher from VF of (111) $\langle uvw \rangle$ fiber but both are decreasing for 1hr and 2hrs conditions in sample 2. At 850°C, VF of (110)

$\langle uvw \rangle$ fiber is increasing till 2hrs then after decreasing and VF of (111) $\langle uvw \rangle$ fiber is decreasing till 2hrs and then after increasing in sample 1. In sample 2, VF of (110) $\langle uvw \rangle$ fiber was decreasing till 850°C, 2hrs; after then it increased till 4hrs. For sample 2, VF of (111) $\langle uvw \rangle$ fiber is increasing slow rate till 2hrs and then after decreasing in case of 850°C.

Table 4.3: volume fraction of gamma fiber, alpha fiber, theta fiber, cube orientation, Goss orientation at different annealed condition in sample 1.

Conditions	(111) $\langle uvw \rangle$: gamma fiber	(100) $\langle uvw \rangle$: α fiber	(110) $\langle uvw \rangle$:fib er	(100) $\langle 001 \rangle$: cube orientation	(110) $\langle 001 \rangle$: Goss orientation
650°C [1hr]	0.0832	0.0363	0.0564	0.0145	0.0153
650°C [2hr]	0.0652	0.037	0.0691	0.0172	0.0175
650°C [4hr]	0.0792	0.0409	0.0809	0.0208	0.0208
750°C [1hr]	0.0294	0.0175	0.0308	0.0077	0.0081
750°C [2hr]	0.0335	0.0222	0.0489	0.0089	0.0148
750°C [4hr]	0.0459	0.0242	0.034	0.0108	0.0091
850°C [1hr]	0.051	0.0488	0.0303	0.0204	0.0106
850°C [2hr]	0.0424	0.0245	0.0523	0.009	0.0145
850°C [4hr]	0.0457	0.0203	0.04	0.011	0.009

Table 4.4: volume fraction of gamma fiber, alpha fiber, theta fiber, cube orientation, Goss orientation at different annealed condition in sample 2.

conditions	(111)<uvw> : gamma fiber	(100)<uvw> : α fiber	(110)<uvw>:fib er	(100)<001> : cube orientation	(110)<001> : goss orientation
650°C [1hr]	0.0714	0.0723	0.0539	0.0299	0.0093
650°C [2hr]	0.1017	0.0392	0.0853	0.0163	0.013
650°C [4hr]	0.074	0.0431	0.0752	0.0195	0.0144
750°C [1hr]	0.0657	0.0394	0.0751	0.0174	0.0156
750°C [2hr]	0.0568	0.0395	0.0685	0.0147	0.0119
750°C [4hr]	0.0584	0.0384	0.07	0.0139	0.0131
850°C [1hr]	0.0505	0.0266	0.0693	0.0122	0.0138
850°C [2hr]	0.0618	0.0273	0.0421	0.0113	0.0062
850°C [4hr]	0.0703	0.0317	0.0842	0.0163	0.0152

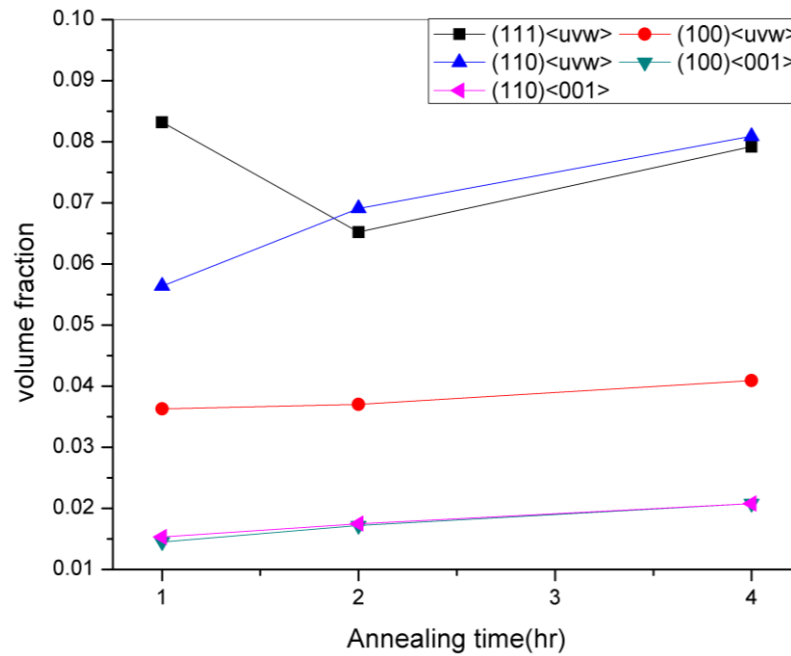


Fig 15(a)

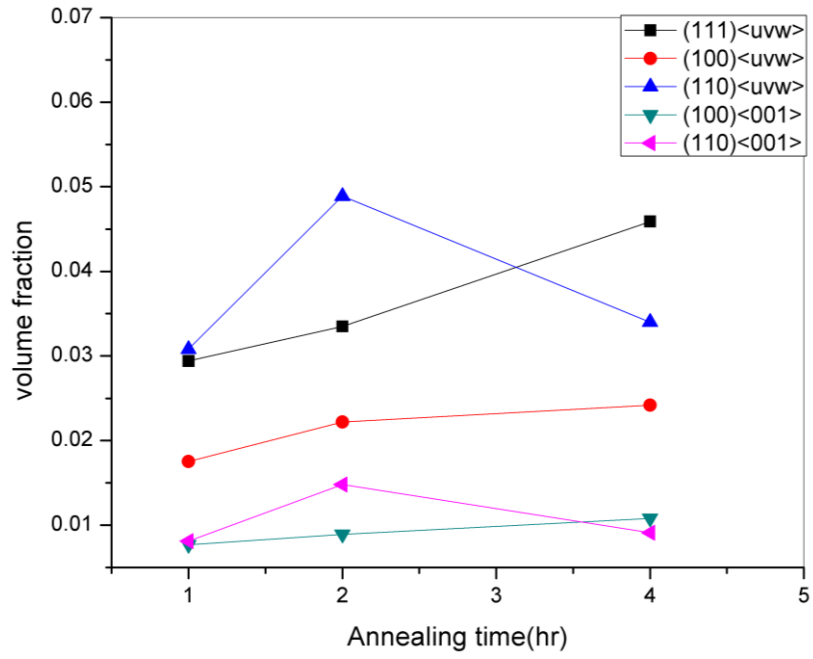


Fig 15(b)

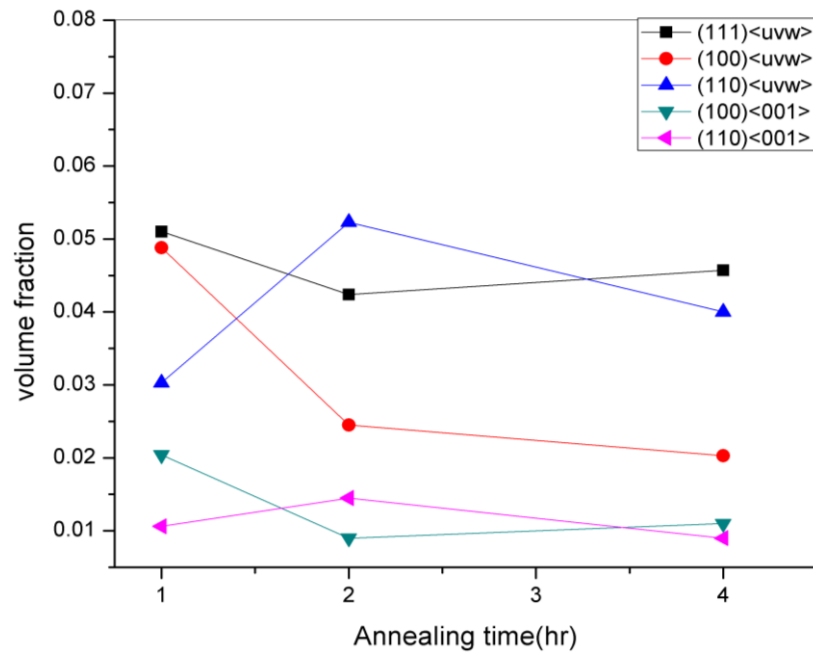


Fig 15(c)

Fig. 4.15: variation of volume fraction of (111) <uvw> { γ fiber}, (110)<uvw> { α fiber}, (100)<uvw> { θ fiber}, (100)<001>{cube orientation},(110)<001>{Goss orientation} of sample 1 annealed at (a) 650°C (b) 750°C (c) 850°C.

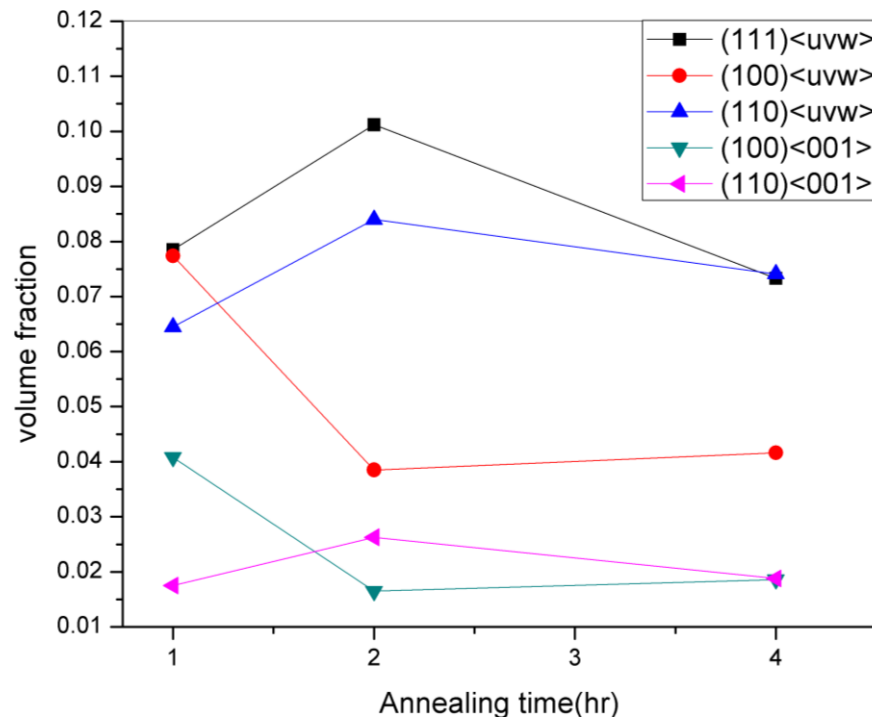


Fig 16(a)

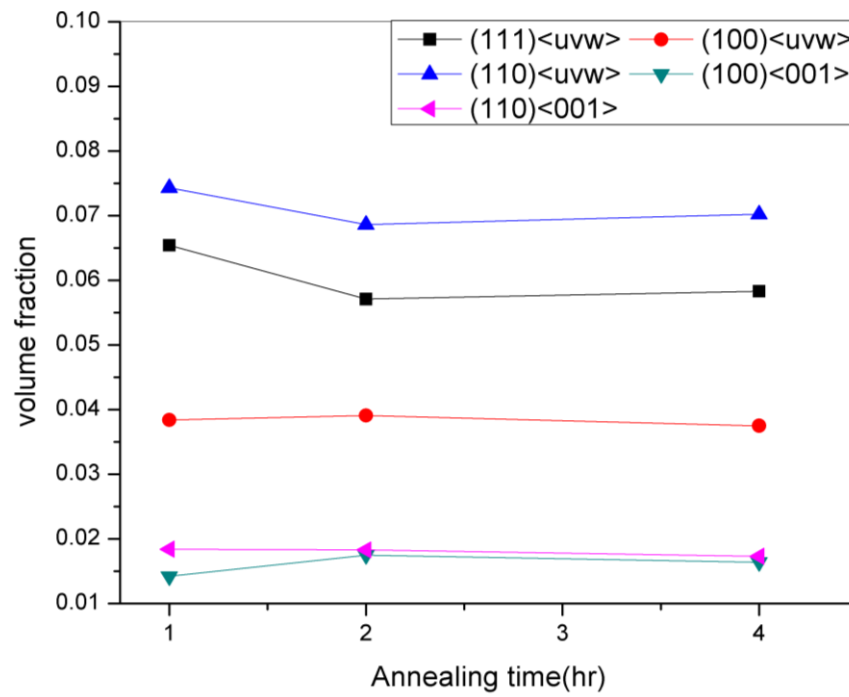


Fig 16(b)

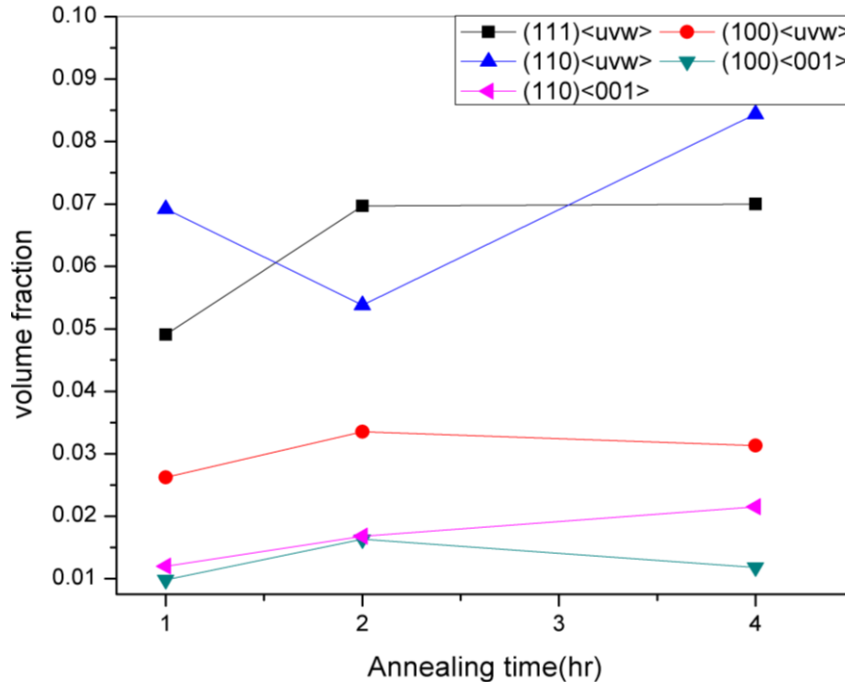


Fig 16(c)

Fig.4.16: : variation of volume fraction of (111) <uvw> { γ fiber}, (110)<uvw> { α fiber}, (100)<uvw> { θ fiber}, (100)<001> {cube orientation}, (110)<001> {Goss orientation} of sample 2 annealed at (a) 650°C (b) 750°C (c) 850°C.

4.1.3 Magnetic properties:

Magnetic properties of sample 1 and sample 2 are shown in figure 4.17 and data are given in table 4.5 and 4.6 at different annealed states. Figures show that core loss is decreasing at faster rate till 2hrs in both sample 1 and sample 2 at 650°C, 750°C and 850°C but rate of degradation of core loss is faster at 850°C in both samples. At 650°C and from 2hrs to 4hrs, core loss is increasing as shown in figure. Except At 650°C and from 2hrs to 4hrs, core loss is decreasing at very slow rate at 750°C and 850°C.

Table 4.5: Core loss at various annealed condition in sample 1.

	650°C	750°C	850°C
1hr	4.966	4.223	4.899
2hrs	3.475	3.362	2.876
4hrs	3.607	3.103	2.713

Table 4.6: Core loss at various annealed condition in sample 2.

	650°C	750°C	850°C
1hr	5.117	4.303	6.567
2hrs	4.533	4.1	3.836
4hrs	4.035	3.96	3.709

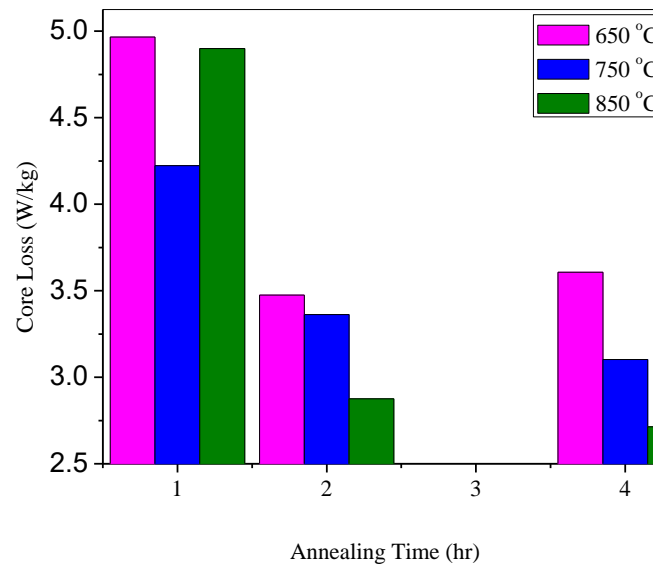


Fig. 4.17(a)

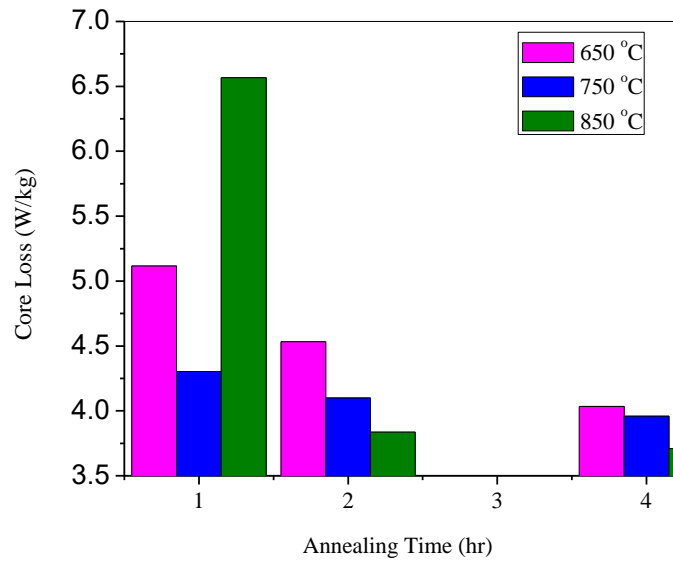


Fig. 4.17(b)

Fig.4.17 Variation core loss (W/kg) with respect to time (hr.) at various temperature (°C) for sample 1 and 2 in figure (a) and (b).

4.2 Discussion:

Chemical composition, crystallographic texture and grain size are the three major factors which are responsible for the magnetic properties of the electrical steels [19, 20, 38, 39]. To increase the resistivity of the steel some elements like P, Si, Al, Mn are mixed with it [40, 41]. The magnetic property of the steels is affected by the major elements i.e., Carbon and Sulfur and that is why the content of these elements should be less in steel for better magnetic properties although this effect can be recovered by second phase precipitation [42, 43]. The alloying elements help in controlling the texture by preventing the growth. Manganese is the best example of growth inhibitor generator for non-oriented steels during annealing [44]. Manganese form MnS during heat treatment of the samples which is helpful to reduce inclusion. This may be the reason for sample 2 of having lower grain size than sample1 in all annealing conditions. It has also come to notice that although sample 1 contains Al which is also a growth inhibitor generator, it shows abnormality in grain growth at high temperature [45]. However, Al has been observed to be harmful for the working efficiency of the samples and this could be resulting in energy

loss during cold rolling which in turn affects the grain growth. Sample 1 has higher grain size and due to this, permeability increases.

During production of steels the thermo-mechanical processes help to control the crystallographic texture and grain size. It has been found that for better magnetic properties of steels, an optimum grain size, lower (111) $\langle uvw \rangle$ fiber and higher other fibers are required [1, 33, 34, 39,]. When VF of (111) $\langle uvw \rangle$ fiber decreases and other fiber increase then samples provide lower core loss. Annealing at longer duration in given temperature, variation in texture is not much more but degradation in core loss happens in slow manner. Because of this reason the produced samples via this process (annealing for the longer time) affect cost economy. Higher grain size means having lower core losses [46]. From the point of view of magnetic property, it was indicated that the abnormality of grain growth was not harmful for sample 1. It has been found that randomized texture is formed in all directions in both samples.

CHAPTER: 5

5.CONCLUSION

5.1 Conclusion:

Microstructure, texture and magnetic properties of CRNO steel having different compositions have been studied and following conclusions can be drawn:

- A sample having higher amount of Aluminium produces abnormal grain growth during annealing of the material.
- A sample having higher amount of Manganese produces normal grain growth during annealing process of the material.
- MSCR and annealing process had significant impact on texture development in the sample. A near equal texture was observed in the samples.
- With an increase in grain size of the samples decreased the core losses in the samples.

REFERENCES

1. B. Verlinder, J. Driver, I. Samajdar, R. D. Doherty, (2007) Thermo-Mechanical Processing Of Metallic Materials, Elsevier Ltd, UK, pp. 428-439.
2. H.Heydari A.Lzadiam, (2008) Phenomena of forward and backward rotation fields respect of localized flux distribution and core losses in single phase induction motor, IEEE Trans. Magn. **58**, pp. 255-265.
3. C.M.B. Bacaltchuk et al, (2003) Effect of magnetic field applied during secondary annealing on texture and grain size of silicon steel, scriptamaterialia, **85**, pp. 1343-1347.
4. R. Prem Kumar, I. Samajdar, N.N. Viswanathan, V. Singal, V. Seshadri (2003) Relative effect(s) of texture and grain size on magnetic properties in a low silicon non-grain oriented electrical steel, J. Magn. & Magn. Mater. **264**, pp. 75-85.
5. V. Randle and O. Engler, (2000) Introduction to Texture Analysis: Macrotexture, Micro Texture and Orientation Mapping, Gordon and Breach Science Publishers. pp. 15-59.
6. A. De Paepe, K. Eloot, J. Dilewijns, and C. Standaert, (1996) Effect of hot rolling parameter on the magnetic properties of a low-silicon ultralow- carbon steel, J. Magn. & Magn. Mater. **160**, pp. 125-135.
7. Amar JaspritDungdung and Rakesh Kumar Sethy, (2014) Textural and Magnetic Properties of Cross-Rolled Silicon Steels, NIT Rourkela.
8. G. Lyudkoushy, P.K. Rastogi, M. Bala, (1986), Non-oriented electrical steel, J. Metals. **22**, pp. 15-24.
9. G. Lyudkoushy, J.M. Shapiro, (1985), J. Appl. Phys. **57** (1), pp. 4235.
10. B. Cornut, A. Kedous-Lebouc, (1996), Th. Waeckerle, J. Magn. Magn. Mater. **160** pp. 98-109.
11. T. Ros-Yanez, Y. Houbaert, (2003), O. Fischer and J. Schneider: Production of High Silicon Steel for Electrical Applications by Thermomechanical Processing, J. Mater. Process. Tech. **141**, pp. 252-259.
12. F. J. G. Landgraf, J. R. F. da Silveira, D Rodrigues-Jr, (2011), determining the effect of grain size and maximum induction upon coercive field of electrical steels, Elsevier, J. Magn. Magn. Mater, **368**, pp. 2335-2339.

13. S.M.Shin, S.Birosca, S.K.Chang, (2008), texture evolution in grain oriented electrical steel during hot band annealing and cold rolling, IEEE Trans. Magn. pp. 460-474.
14. Youliang He, Erik J. Hilinski, (2016), Texture and magnetic properties of non-oriented electrical steels processed by an unconventional cold rolling scheme, J. Magn.&Magn. Mater, **204**, pp. 337-352.
15. M. Rout, S. K. Pal and S. B. Singh, (2015), Cross Rolling: A Metal Forming Process, pp. 41-64.
16. Steel statistical yearbook, (2009), World Steel Association, World steel Committee on Economic Studies, Brussels, pp. 50-64.
17. B. D. Cullity, C.D. Graham, (2009), Introduction to Magnetic Materials, 2nd Edition, John Wiley & Sons, **23**, pp. 432-447.
18. D. Prusty, H.K. Pradhan, (2012), An Investigation on Texture Property Correlation in Cold Oriented Silicon Steels, National Institute of Technology, Rourkela.
19. Jae Kyoun Kim, (2014), the evolution of the goss and cube textures in electrical steel, materials letters, **56**, pp. 110-113.
20. Wenk H.-R., (1985), Preferred Orientation in Deformed Metals and Rocks: An Introduction to Modern Texture Analysis, Academic Press, and Orlando **24**, pp. 54-68.
21. <http://crgosteel.com/index.htm>.
22. Roger D. Doherty and Surya R. Kalidindi, (2008), Microstructure Evolution in Deformed and Recrystallized Electrical Steel, Dejan Stojakovic, **33**, pp. 325-389.
23. Aernoudt E., Van Houtte P. Leffers T., (1993), Deformation and textures of metals large strain, in Materials Science and Technology, R.W. Cahn (ed.), **6**, pp. 74-89.
24. Satyam Suwas AND Nilesh P. Gurao, (2008), Crystallographic texture in Materials, journal.lib.Iisc, pp. 224-238.
25. C. Maddison, (2008), Generators: Improvements and New Developments – Requirements on Electrical Steels, Proceedings of 3rd International, Conference on Magnetism and Metallurgy, Ghent University, Gent-Zwijnaarde, pp. 35-38.
26. Ray RK, Jonas JJ, (1990), Transformation textures in steels, Int Mater, **35**, pp. 1–36.
27. S. Suwas and R. K. Ray, (2014), Crystallographic Texture of Materials, Springer, pp. 10-22.
28. J.A. Szpunar, in: H.J. Bunge (Ed.), (1988), Texture, Anisotropy in Magnetic Steels, Direction Properties of Materials, CuvllierVerlag, Gttingen, **13**, pp. 124-134.

29. Bessieres, J., Heizmann, J.J. and Eberhardt, A, (1991), Textures and Microstructures, **23**, pp. 153-159.
30. Bunge HJ, (1965) Zur Darstellung allgemeiner texture. Z Metallkd, **5**, pp. 872–874.
31. Roe RJ, (1965), Description of crystallite orientation in polycrystalline materials. III. General solution to pole figure inversion. J Appl Phys. **8**, pp. 2024–2031.
32. M. Rout, S. K. Pal and S. B. Singh, (2015), Cross Rolling: A Metal Forming Process, pp. 41-64.
33. Yasihiki H. Okamoto, (1987), Effect of hot band grain size on magnetic properties of non-oriented electrical steels, IEEE Trans Magn, **23**, pp. 3086–3088.
34. H. Yasihiki and Okamoto, (2002), Effect of hot band grain size on magnetic properties of nonoriented electrical steels, IEEE Trans. Magn. **23**, pp. 3086.
35. B. Verlinder, J. Driver, I. Samajdar, R. D. Doherty, (2007) Thermo-Mechanical Processing Of Metallic Materials, Elsevier Ltd, UK, pp. 428-439
36. K.Pawlik, P.Ozga, (1999), LaboTex: the texture analysis software, Gottinger Arbeitszue zur Geologie und Palaontologie, SB4.
37. Helmut Brockhaus, Dinslaken, (2007), Method for Operating a Measuring Instrument, patent no: US7171336 B6.
38. K. Matsumura, B. Fukuda, (1984), Magnetic Materials in Japan: Research, Applications and Potential IEEE Trans. Magn. MAG-20, **5**, pp. 1533-1554.
39. M.F. de Campos, J.C. Teixeira, F.J.G. Landgraf, (2006), the optimum grain size for minimizing energy losses in iron, J. Magn. & Magn. Mater. **235**, pp. 94-99.
40. C. J. Van Tyne, (2014), Comprehensive Materials Processing, **13**, pp. 198-208.
41. Yuqing Weng, (2011), Advanced Steels: The Recent Scenario in Steel Science and Technology, the Chinese society for metals, Beijing, pp. 116-128.
42. S. Nishijima and S. Iwata, (1997), computerization and networking of material databases, **4**, pp. 8-13.
43. K. C. Liao, (1986), the effect of manganese and sulfur contents on the magnetic properties of cold rolled lamination steels, Technical Centers, National Steel Corporation, **18**, pp. 1259-1266.
44. Taisei Nakayama, Noriyuki Honjou, Takashi Minaga, Hiroyoshi Yashiki, (2001), Effects of manganese and sulfur contents and slab reheating temperatures on the magnetic properties of non-oriented semi-processed electrical steel sheet, J. Magn. & Magn. Mater, **123**, pp. 55-61.

45. Rodrigo Felix de Araujo Cardoso, Luiz Brandao, Marco Antônio da Cunha, (2008), Influence of Grain Size and Additions of Al and Mn on The Magnetic Properties of Non-Oriented Electrical Steels With 3 wt. (%) Si, *Materials Research*, **68**, pp. 51-55.
46. A.C. Marco and C.P. Sebastian, (2003), Effect of the Annealing Temperature on the Structure and Magnetic Properties of 3% Si Non-oriented Steel, *J. Magn. Magn. Mater*, **145**, pp. 379–381.